In presenting the dissertation as a partial fulfillment of the requirements for an advanced degree from the Georgia Institute of Technology, I agree that the Library of the Institute shall make it available for inspection and circulation in accordance with its regulations governing materials of this type. I agree that permission to copy from, or to publish from, this dissertation may be granted by the professor under whose direction it was written, or, in his absence, by the Dean of the Graduate Division when such copying or publication is solely for scholarly purposes and does not involve potential financial gain. It is understood that any copying from, or publication of, this dissertation which involves potential financial gain will not be allowed without written permission.

_____ 6/3/68

3/17/65
b

THEORETICAL AND EXPERIMENTAL DETERMINATION OF DYNAMIC STRESSES IN ELASTICALLY ISOTROPIC FLAT PANELS SUBJECTED TO SINUSOIDAL VIBRATORY LOADING

A THESIS

Presented to

the Faculty of the Graduate Division

by

Cecil William Schneider

In Partial Fulfillment of the Requirements

for the Degree

Master of Science in Engineering Mechanics

Georgia Institute of Technology

May, 1968

THEORETICAL AND EXPERIMENTAL DETERMINATION OF DYNAMIC STRESSES IN ELASTICALLY ISOTROPIC FLAT PANELS SUBJECTED TO SINUSOIDAL VIBRATORY LOADING

Approved:

Thesis Advisor

Date Approved by Chairman: 5-24-68

ACKNOWLEDGMENTS

The author wishes to thank the many persons whose combined efforts have made this thesis possible.

The author is especially indebted to Dr. M. C. Bernard for his guidance during the investigation.

Dr. D. J. McGill, Dr. C. E. S. Ueng and Dr. E. R. Wood of the advisory committee are thanked for their helpful comments and advice.

Special thanks are also due for the assistance of the Lockheed-Georgia Company, Marietta, Georgia, in providing the test facilities for conducting the experimental portion of this study. Mr. H. F. Hunter of the Aeromechanics Division is thanked for his helpful comments and advice during the research.

The author is indebted to Mrs. R. D. Bowen for her generous contribution in typing this thesis.

And last, but not least, the author would like to express sincerest appreciation to his wife for her continued encouragement and patience during this study.

TABLE OF CONTENTS

LIST OF TABLES

LIST OF ILLUSTRATIONS

LIST OF ILLUSTRATIONS (CONT'D)

LIST OF ILLUSTRATIONS (CONT'D)

SUMMARY

Analytical expressions were derived to calculate dynamic stresses and damped natural frequencies in flat panels subjected to a uniform lateral boundary displacement. Both simply supported and clamped boundary conditions were considered in the analysis.

A test program was conducted on a 9 by 11 inch panel subjected to mechanical vibratory loading. Natural frequencies and dynamic stresses were measured for the first four symmetric modes of vibration. The analytical and test results were compared, and the analytical equations were then modified to yield empirical dynamic stress functions.

A parameter study was conducted to show the range of the natural frequency and maximum stress using typical panel values. Figures are presented showing the effect of varying panel parameters on dynamic stress and natural frequency.

NOTATION

A	Coefficient of deflection function
a	Length of panel in x-direction ~ in.
b	Length of panel in y-direction ~ in.
C	Equivalent Viscous Damping coefficient ~ lb.-sec./in.^{3}
C_c	Critical damping coefficient ~ lb.-sec./in.^{3}
D	Panel flexural rigidity = $\frac{Eh^3}{12(1-\nu^2)}$ ~ in.-lb.
E	Modulus of elasticity ~ psi
f	Frequency ~ Hz
g	Transient response of panel ~ in.
G	Acceleration of gravity ~ in./sec.^{2}
h	Panel thickness ~ in.
Hz	Hertz ~ cycles/second
K_{mr}, K_{ns}	Non-dimensional parameters used in the clamped panel analysis
m,n,r,s	Modal summation indices
N	Truncation value for series solution
psi	Pounds per square inch
q	Applied lateral load ~ psi
rms	Root mean square
SG	Strain Gage
t, T	Time ~ sec.

U_m, V_n	Non-dimensional parameters used in the clamped panel analysis
w	Transverse panel displacement ~ in.
W	Panel mode shape
W_{mn}	Eigenfunctions of the panel; assumed modal functions
x,y,z	Rectangular coordinates
α	Constant of proportionality in damping coefficient coefficient ~ lb./in.^{3}
α_m, θ_n	Non-dimensional parameters used in the clamped panel analysis
β_m, γ_n	Parameters used in the clamped panel analysis ~ in.$^{-2}$
δ	Kronecker delta
ϵ	Orthogonality constant of integration
ζ	Damping factor - ratio of actual to critical damping coefficients
η^4	Eigenvalue for free vibration ~ in.$^{-4}$
λ^4	Frequency parameter ~ in.$^{-4}$
ν	Poisson's Ratio
ξ	Displacement of panel boundary from reference plane ~ in.
ρ	Panel mass density ~ lb.-sec.^{2}/in.^{4}
σ	Dynamic stress ~ psi
τ	Phase angle ~ rad.
ϕ_m, ψ_n	Mode shapes for the clamped panel
ω	Circular frequency ~ rad./sec.
ω_{mn}	Undamped natural frequency ~ rad./sec.

Ω_{mn}	Damped natural frequency ~ rad./sec.
∇	Del operator

Superscript

$\cdot$	Differentiation with respect to time

Subscript

m,n,r,s	Modal indices
x,y	Partial differentiation with respect to x,y
o	Static equilibrium value
x-x, y-y	Direction of stress vector

Matrices

$[D]$	Pseudo-dynamical matrix
$[I]$	Identity matrix
$\{P\}$	Input matrix
$[Z]$	Frequency-response matrix

CHAPTER I

INTRODUCTION

The purpose of this research is to determine the dynamic stresses in flat elastic panels under harmonic motion for both simply supported and clamped edges. The results of the analysis are compared with test data to modify the dynamic stress functions.

In a typical aircraft structural installation the edges of the flat panel are restrained elastically. However, the analysis of a panel with elastically supported edges becomes unduly complex in view of the uncertainties involved in selecting values for the elastic constraints used in the analysis. The analysis presented herein for the clamped and simply supported panel provides upper and lower bounds for the actual natural frequencies and dynamic stresses encountered in a typical structural panel supported by stiffeners which are relatively rigid in bending but will allow some rotation.

The flat panel has been covered quite extensively in the literature with regard to natural frequency and mode shape determination under various boundary conditions. However, very little attention has been given to evaluating the dynamic stresses under vibratory loading. Those authors discussing dynamic stresses usually restrict the analysis to the maximum stress (e.g., at the side of the plate for the clamped plate) existing in the fundamental mode. This research extends the classical modal analysis to obtain dynamic stress

functions valid for the entire panel domain. The analysis covers all symmetric modes and is therefore not restricted by the usual assumption that all fatigue damage is incurred from the stress in the fundamental mode.

S. Tomotika [1] was among the first authors to present a formal solution for the transverse vibration of a square plate with all edges clamped. He formulated the displacement to satisfy both the boundary conditions and the differential equation of transverse vibration and carried out the numerical effort for the fundamental mode of the square plate.

Young[2] used the functions defining the normal modes of vibration of a uniform beam and the Ritz Method to determine the natural frequencies and modes of vibration of a square plate with clamped edges and two combinations of clamped and free edges. Numerical data were presented for the first six modes of vibration for the square plate clamped on all edges.

Warburton[3] determined the frequencies of free transverse vibration of rectangular isotropic plates for all combinations of free, simply supported and clamped edges. He derived an approximate frequency formula by applying the Rayleigh Energy Method and assuming that the waveforms of vibrating plates were similar to those of vibrating beams. The frequency was expressed in terms of the boundary conditions, the modal pattern, the dimensions of the plate, and the material constants. Results were presented as a table of frequency parameters for 15 boundary conditions. A lengthy discussion of degenerate modes was also included.

The method of M. Levy[4] was used by Huffington and Hoppmann[5] to obtain frequency equations and modal eigenfunctions for flexural vibrations of rectangular orthotropic plates. Simply supported, clamped and free edges were considered and characteristic frequency equations and modal functions were presented for seven cases of mixed boundary conditions, excluding the plate clamped on all edges.

Hearmon[6] extended Warburton's[3] analysis to cover vibration of orthotropic plates with any combination of simply supported or clamped edges. Frequency parameters were shown to be nearly identical to those obtained by Reference (5).

In his thesis, Ballal[7] presented numerical data for natural frequencies of rectangular plates with all possible combinations of simply supported, clamped and free edges. Levy's method and the Ritz energy minimization procedure were utilized in this analysis.

Laura and Saffell[8] employed the Galerkin Method to analyze the vibration of the clamped rectangular plate. A simple polynomial approximation was used to represent the plate deflection. A table of frequency coefficients was presented for the first four modes. The results of the analysis showed very good agreement with the work of other authors.

Ford [9] and Mercer and Seavey[10] calculated natural frequencies and normal modes of a row of skin-stringer panels. Ford conducted tests under acoustic loading which showed order of magnitude agreement with the theoretical results.

Lin[11] expanded an earlier analysis[12] to determine stresses in continuous skin-stringer panels subjected to random loading. The

maximum root-mean-square stress values were computed for a typical structural configuration and showed general agreement with measured data.

Clarkson[13] presented a simplified flat plate response theory based on a uni-modal response resembling a single degree-of-freedom oscillator to determine stresses induced by acoustic pressure. The analytical estimates were within a factor of two of the measured data.

Ballentine, Rudder, Mathis and Plumblee[14] developed relations to calculate natural frequencies and maximum stresses for flat panels in the fundamental mode considering simply supported and clamped edges. Extensive test data was compiled into design nomographs; however the primary emphasis was on acoustic fatigue requirements, and hence the analysis was conducted only to point out the necessary parameters on which to base the design charts.

CHAPTER II

ANALYSIS

Natural frequencies and mode shapes in flat panels may be determined by use of several exact or approximate methods. The choice of method of analysis is based on a consideration of the degree of accuracy desired, the amount of labor involved to achieve the solution, the type of boundary conditions considered, etc. The analysis presented herein utilizes modal expansions to obtain the natural frequencies, mode shapes and dynamic stresses.

General

It is assumed that the panel material is linearly elastic, homogenous and isotropic, and that the classical assumptions for bending of a thin plate with no in-plane forces are valid; i.e.,

(1) The deflection of the plate is small compared to the thickness, while the plate thickness is small compared to the surface dimensions.

(2) There is no resultant force on the cross-sectional area of a plate element. Hence, there is no deformation in the middle plane of the plate during bending and this plane is a neutral plane.

(3) Any straight line normal to the middle plane before deformation remains a straight line normal to the neutral plane during deformation.

(4) The normal stresses in the direction transverse to the plate can be neglected.

The panel configuration and rectangular coordinate system used in the analysis are shown in Figure 1. The x, y, z coordinate system coincides with the middle surface of the plate at equilibrium, and the deflection surface w(x,y;t) is referred to this plane.

Equation of Motion

The differential equation for forced vibration of a thin plate may be determined from a consideration of the energy in the plate and an application of Lagrange's Equations. The equation of motion is derived in many texts on elasticity and vibration and, assuming equivalent viscous damping, has the form

$$D\nabla^4 w(x,y;t) + C\dot{w}(x,y;t) + \rho h\ddot{w}(x,y;t) = q(x,y;t) \qquad (1)$$

Free Vibration

Consider first the free vibration case in which the governing equation becomes

$$\nabla^4 w + \frac{C}{D}\dot{w} + \frac{\rho h}{D}\ddot{w} = 0 \qquad (2)$$

Assume that the solution of the above is separable in time and space and of the form

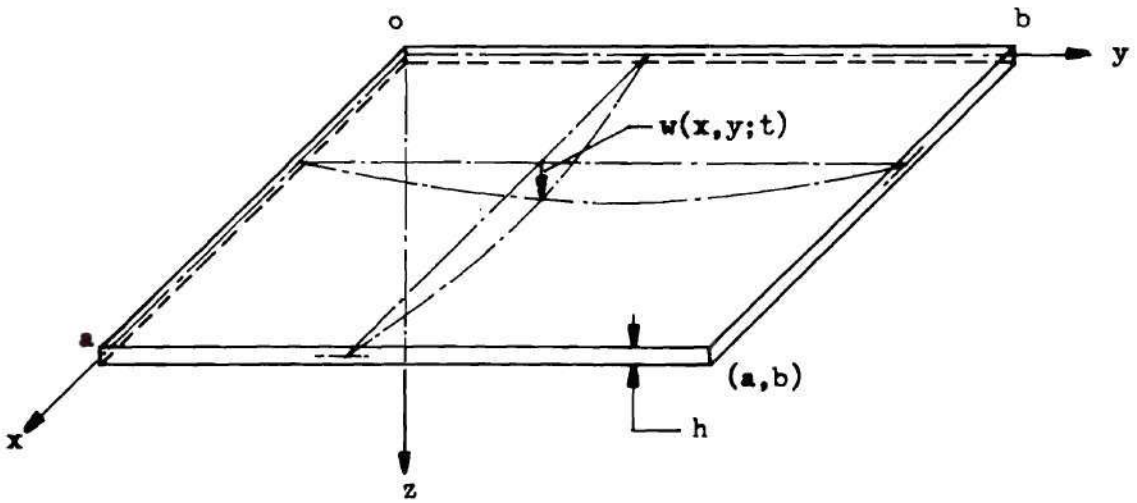

Figure 1. Panel Configuration and Coordinate System

$$W(x,y;T) = W(x,y)\, g(T) \tag{3}$$

Introducing expression (3) into equation (2) and dividing through by Wg yields

$$\frac{\nabla^4 W}{W} = -\frac{1}{g}\left(\frac{C}{D}\dot{g} + \frac{\rho h}{D}\ddot{g} \right) = \eta^4 \tag{4}$$

where η^4 is the eigenvalue and is a constant. The above equation is possible since W depends only on x and y, while g is dependent only on t.

Separation of equation (4) results in the classical eigenvalue problem for the flat plate and the harmonic response equation, or

$$\nabla^4 W_{mn} - \eta_{mn}^4 W_{mn} = 0 \tag{5}$$

$$\frac{\rho h}{D}\ddot{g}_{mn} + \frac{C}{D}\dot{g}_{mn} + \eta_{mn}^4 g_{mn} = 0 \tag{6}$$

The solution of the eigenvalue problem (5) is dependent on the boundary conditions of the plate and will be covered later in this chapter.

The solution of the second order differential equation (6) is easily found, and for damping less than critical ($\zeta < 1$), is given by

$$q_{mn}(T) = A\, e^{-(C/2\rho h)T} \sin\left[\sqrt{\frac{\eta_{mn}^4 D}{\rho h} - \frac{C^2}{4\rho^2 h^2}}\; T + \tau_{mn}\right] \tag{7}$$

The above equation represents the transient response of the plate and is identical to the transient response of a simple damped oscillator. Therefore, by comparison, the natural frequency of damped oscillation may be written as

$$\Omega_{mn} = \sqrt{\frac{\eta_{mn}^4 D}{\rho h} - \frac{C^2}{4\rho^2 h^2}} \tag{8}$$

Forced Vibration

Under arbitrary forced vibration, the response of the panel is governed by equation (1), where the forces q(x,y;t) are lateral loads applied directly to the panel.

This analysis will be restricted to panel excitation produced by a uniform lateral displacement of the boundaries

$$\xi(T) = \xi_0\, e^{i\omega T} \tag{9}$$

where ξ is the displacement of the panel boundary from a fixed reference plane, as shown in Figure 2. The reference plane is at a distance ξ_o from the panel mid-plane at equilibrium. The bending strain energy and damping forces in the panel are unaltered by this coordinate translation since they are dependent on the relative displacement w. However, the kinetic energy must be determined from the absolute velocity of the panel in the deformed position, or

$$\dot{\xi} + \dot{w}$$

Since the inertia term results directly from the kinetic energy the equation of motion may be appropriately modified to include the boundary displacement. This results in

$$D\nabla^4 w + C\dot{w} + \rho h(\ddot{\xi} + \ddot{w}) = 0$$

The right side of the above equation is zero since there are no loads applied directly to the plate. Rearranging the above equation gives

$$D\nabla^4 w + C\dot{w} + \rho h\ddot{w} = -\rho h\ddot{\xi} \qquad (10)$$

Where $\ddot{\xi}$ is the acceleration of the panel boundary.

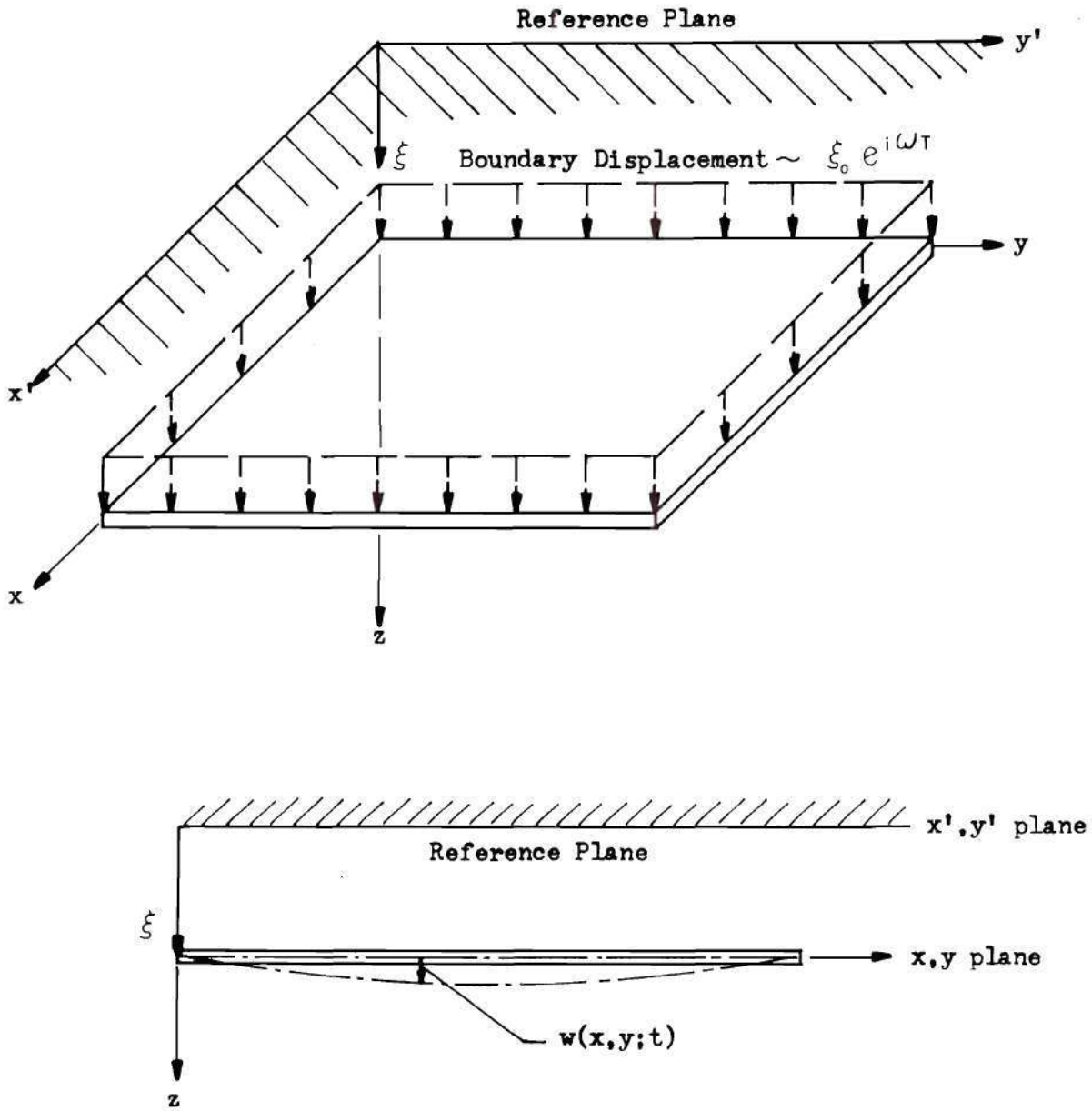

Figure 2. Boundary Forces and Reference Plane Coordinates

Since the input displacement is harmonic in time, assume that the response is also harmonic. Thus take

$$W(x,y;T) = W(x,y)\, e^{i(\omega T - \tau_{mn})} \tag{11}$$

Substitution of expressions (9) and (11) into the equation of motion yields

$$\nabla^4 W - \lambda^4 W = \frac{\rho h \xi_0 \omega^2}{D} e^{i\tau_{mn}} \tag{12}$$

where

$$\lambda^4 = \left(\frac{\omega^2 \rho h}{D} - i \frac{C\omega}{D} \right) \tag{13}$$

Equation (12) is then the general expression for the steady-state response of a panel subjected to a harmonic boundary displacement.

Boundary Conditions

The boundary conditions for the simply supported and clamped panels used in this analysis are stated as follows:

Simply-Supported Panel

$$W(0,y) = W(a,y) = W(x,0) = W(x,b) = 0 \tag{14}$$

$$W_{xx}(0,y) = W_{xx}(a,y) = W_{yy}(x,0) = W_{yy}(x,b) = 0 \tag{14a}$$

Clamped Panel

$$W(0,y) = W(a,y) = W(x,0) = W(x,b) = 0$$

$$W_x(0,y) = W_x(a,y) = W_y(x,0) = W_y(x,b) = 0 \tag{15}$$

The above equations represent the classical boundary conditions of zero displacement and moment on the edges of the simply supported panel and zero displacement and slope at the edges of the clamped panel.

Simply Supported Panel

The eigenvalue equation for the free vibration of a flat panel is given by equation (5). The eigenvalue problem may be solved exactly by imposing the boundary conditions (14) for the simply supported panel. This boundary value problem is solved in most vibration texts (e.g., Nowacki[15]) and yields the eigenfunctions

$$W_{mn} = \sin\frac{m\pi x}{a} \sin\frac{n\pi y}{b} \tag{16}$$

Since these eigenfunctions identically satisfy the boundary value problem, they form a complete set, and may be expanded in an absolutely and uniformly convergent series to represent the displacement.

Natural Frequencies

From the solution to the boundary value problem, the eigenvalue η_{mn}^4 is determined to be the square of the sum of the squares of the arguments of the sine functions, or

$$\eta_{mn}^4 = \pi^4 \left[\left(\frac{m}{a}\right)^2 + \left(\frac{n}{b}\right)^2 \right]^2$$

Substitution of this expression into equation (8) gives the damped natural frequency

$$\Omega_{mn} = \left[\pi^4 \left(\frac{m^2}{a^2} + \frac{n^2}{b^2} \right)^2 \frac{D}{\rho h} - \frac{C^2}{4\rho^2 h^2} \right]^{1/2}$$

The first term in the bracket is recognized as the square of the natural frequency of undamped vibration for the simply supported panel. To simplify the above equation, the damping may be expressed in terms of a non-dimensional damping factor by substituting

$$C = \frac{\alpha}{\pi \omega} \tag{17}$$

for the equivalent viscous damping coefficient from Reference (16). The critical damping coefficient is defined as the value of damping coefficient which reduces the radical in expression (7) to zero, and the damping factor

is given by the ratio of actual damping to critical damping coefficients. Thus

$$\zeta = \frac{\alpha}{2\pi\omega\rho h\omega_{mn}} \tag{18}$$

The damped natural frequency then simplifies to

$$\Omega_{mn} = \omega_{mn}\sqrt{1-\zeta^2} \tag{19}$$

where the undamped natural frequency is equal to

$$\omega_{mn} = \pi^2\left(\frac{m^2}{a^2}+\frac{n^2}{b^2}\right)\sqrt{\frac{D}{\rho h}} \tag{20}$$

The preceding relation is similar to the single degree-of-freedom damped oscillator case, and relates the oscillation of damped vibration to the undamped natural frequencies.

Forced Vibration

To evaluate the steady-state response of the simply supported panel subjected to harmonic boundary displacements, expand the deflection into a series of the eigenfunctions W_{mn} of free vibration.

$$W(x,y) = \sum_{m=1}^{\infty}\sum_{n=1}^{\infty} A_{mn}W_{mn}(x,y) \tag{21}$$

By multiplying both sides of equation (12) by W_{rs} and integrating over the domain, the relation

$$\int_0^a\int_0^b [\nabla^4 W - \lambda^4 W] W_{rs}\, dX\, dY = \frac{\rho h \xi_o \omega^2}{D} e^{i\tau_{mn}} \int_0^a\int_0^b W_{rs}\, dX\, dY \tag{22}$$

is obtained. The orthogonality condition for the eigenfunction is

$$\int_0^a\int_0^b W_{mn} W_{rs}\, dX\, dY = \epsilon_{mn} \delta_{mr} \delta_{ns} \tag{23}$$

where δ is the Kronecker delta and ϵ is the orthogonality constant of integration. Substituting equation (21) and recalling that

$$\nabla^4 W_{mn} = \eta_{mn}^4 W_{mn}$$

from equation (5), equation (22) becomes

$$\int_0^a\int_0^b \left[\nabla^4 \left(\sum_m \sum_n A_{mn} W_{mn}\right) - \lambda^4 \left(\sum_m \sum_n A_{mn} W_{mn}\right)\right] W_{rs}\, dX\, dY = \frac{\rho h \xi_o \omega^2}{D} e^{i\tau_{mn}} \int_0^a\int_0^b W_{rs}\, dX\, dY$$

Applying the orthogonality condition yields

$$A_{rs}\left(\eta_{rs}^4 - \lambda^4\right)\epsilon_{mn} = \frac{\rho h \xi_o \omega^2}{D} e^{i\tau_{mn}} \int_0^a \int_0^b W_{rs}\, dX\, dY$$

or

$$A_{mn} = \frac{4\rho h \xi_o \omega^2}{ab D\left(\eta_{mn}^4 - \lambda^4\right)} e^{i\tau_{mn}} \int_0^a \int_0^b W_{mn}\, dX\, dY$$

Inserting the eigenfunctions, the above simplifies to

$$A_{mn} = \begin{cases} \dfrac{16\,\xi_o \omega^2}{mn\,\pi^2 \omega_{mn}^2} \dfrac{1}{\sqrt{\left[1 - (\omega/\omega_{mn})^2\right]^2 + \left[2\zeta\,\omega/\omega_{mn}\right]^2}} & \text{(m,n odd)} \\ 0 & \text{(m,n even)} \end{cases} \qquad (24)$$

Since A_{mn} exists only for odd values of m and n, only the symmetric modes will be excited. The phase angle between the input and the panel response is found to be

$$\tau_{mn} = TAN^{-1}\left[\frac{2\zeta\,\omega/\omega_{mn}}{1 - (\omega/\omega_{mn})^2}\right] \qquad (25)$$

For convenience in comparison with the measured data, the absolute boundary displacement may be replaced by

$$\xi_o = \ddot{\xi}/\omega^2 \tag{26}$$

Substituting equations (16), (21), (24), (25) and (26) into the displacement relation (11) yields the final deflection of the panel.

$$W(X,Y,T) = \frac{16\,\ddot{\xi}}{\pi^2} \sum_{\substack{m \\ odd}} \sum_{n} \frac{e^{i(\omega T - \tau_{mn})}\, SIN\frac{m\pi X}{a}\, SIN\frac{n\pi Y}{b}}{mn\,\omega_{mn}^2 \sqrt{\left[1-(\omega/\omega_{mn})^2\right]^2 + \left[2\zeta\,\omega/\omega_{mn}\right]^2}} \tag{27}$$

Dynamic Stresses

The dynamic stresses may be conveniently expressed in terms of the panel displacement provided the eigenfunctions comprising the displacement are twice differentiable within the domain of the panel, ($0 \le x \le a$; $0 \le y \le b$). Uniform covergence and therefore differentiability of the displacement is assured, since the panel domain is within the interval of convergence of the eigenfunctions.

The stress equations may be written in terms of the displacement w and the lateral distance z from the neutral plane. From small displacement theory, the stresses parallel to the coordinate axes (x,y) are given by Timoshenko[17] as

$$\sigma_{X\text{-}X} = -\frac{E\,z}{(1-\nu^2)}\left(W_{XX} + \nu\, W_{YY}\right) \quad ; \quad \sigma_{Y\text{-}Y} = -\frac{E\,z}{(1-\nu^2)}\left(W_{YY} + \nu\, W_{XX}\right) \tag{28}$$

Since the stresses involve only differentiation with respect to the spatial variables (x,y) the above equation may be written in terms of the eigenfunctions W_{mn}.

$$\sigma_{X\text{-}X} = -\frac{E\,z}{(1-\nu^2)} \sum_{m\,\text{odd}} \sum_{n} A_{mn}\left(W_{mn_{XX}} + \nu\, W_{mn_{YY}}\right) e^{i(\omega T - \tau_{mn})}$$

$$\sigma_{Y\text{-}Y} = -\frac{E\,z}{(1-\nu^2)} \sum_{m\,\text{odd}} \sum_{n} A_{mn}\left(W_{mn_{YY}} + \nu\, W_{mn_{XX}}\right) e^{i(\omega T - \tau_{mn})}$$

Performing the indicated differentiation, the relation

$$\sigma_{X\text{-}X} = \frac{E\,z}{(1-\nu^2)} \sum_{m\,\text{odd}} \sum_{n} A_{mn}\pi^2 \left(\frac{m^2}{a^2} + \nu\,\frac{n^2}{b^2}\right) W_{mn}\, e^{i(\omega T - \tau_{mn})}$$

$$\sigma_{Y\text{-}Y} = \frac{E\,z}{(1-\nu^2)} \sum_{m\,\text{odd}} \sum_{n} A_{mn}\pi^2 \left(\frac{m^2}{a^2} + \nu\,\frac{n^2}{b^2}\right) W_{mn}\, e^{i(\omega T - \tau_{mn})}$$

is obtained. The maximum stress amplitude at any point (x,y) in the panel occurs at the surface

$$z = \pm\, h/2$$

Hence, the dynamic stresses at any point (x,y) in a panel subjected to uniform boundary loading are given by

$$\sigma_{X\text{-}X} = \frac{8 E h \ddot{\xi}}{1-\nu^2} \sum_{\substack{m \\ odd}} \sum_{n} \left\{ \frac{n\left[\left(\frac{m}{n}\right)^2 + \nu\left(\frac{a}{b}\right)^2\right] \text{SIN}\frac{m\pi x}{a} \text{SIN}\frac{n\pi y}{b}}{m a^2 \omega_{mn}^2 \sqrt{\left[1-(\omega/\omega_{mn})^2\right]^2 + \left[2\zeta\omega/\omega_{mn}\right]^2}} \right\} e^{i(\omega T - \tau_{mn})} \tag{28}$$

$$\sigma_{Y\text{-}Y} = \frac{8 E h \ddot{\xi}}{1-\nu^2} \sum_{\substack{m \\ odd}} \sum_{n} \left\{ \frac{n\left[\left(\frac{a}{b}\right)^2 + \nu\left(\frac{m}{n}\right)^2\right] \text{SIN}\frac{m\pi x}{a} \text{SIN}\frac{n\pi y}{b}}{m a^2 \omega_{mn}^2 \sqrt{\left[1-(\omega/\omega_{mn})^2\right]^2 + \left[2\zeta\omega/\omega_{mn}\right]^2}} \right\} e^{i(\omega T - \tau_{mn})}$$

The above equations determine the dynamic stresses occuring in the panel at any instant of time. The stress vectors are in phase with the panel displacement and lag the input by the phase angle τ_{mn}, which becomes 90^o at resonance ($\omega = \omega_{mn}$). For a given input frequency ω the stresses consist of contributions from each of the modes (m,n), each modal contribution being a function of the ratio between the forcing frequency ω and the natural frequency ω_{mn}.

At the condition of resonance the stress component in the excited mode predominates, hence the modal stresses may be approximated by discarding the summation.

$$\sigma_{X\text{-}X_{mn}} = \frac{4 E h \ddot{\xi}}{a^2(1-\nu^2)\zeta\omega_{mn}^2} \left(\frac{n}{m}\right)\left[\left(\frac{a}{b}\right)^2 + \nu\left(\frac{m}{n}\right)^2\right] \text{SIN}\frac{m\pi x}{a} \text{SIN}\frac{n\pi y}{b}\, e^{i(\omega T - \pi/2)} \tag{29}$$

$$\sigma_{Y\text{-}Y_{mn}} = \frac{4 E h \ddot{\xi}}{a^2(1-\nu^2)\zeta\omega_{mn}^2} \left(\frac{n}{m}\right)\left[\left(\frac{m}{n}\right)^2 + \nu\left(\frac{a}{b}\right)^2\right] \text{SIN}\frac{m\pi x}{a} \text{SIN}\frac{n\pi y}{b}\, e^{i(\omega T - \pi/2)} \tag{30}$$

The stresses calculated for the first mode by means of the above approximation were within 0.03% of the values given by the sum of the first nine terms of the series (28). Hence the simplification obtained by neglecting the remaining terms of the series is justified.

As an additional check on the rate of convergence of the dynamic stresses, the values of the stresses were calculated for frequencies of 50 and 200 Hz, which do not coincide with any of the natural frequencies. Figures 3 and 4 depict the results of these calculations. At 50 Hz the values after summing nine terms of the series were within 0.4% of the 16 term solution. At 200 Hz the stresses after nine terms were within 11% of the 16 term solution. However, the off-resonance stresses occurring at 50 and 200 Hz are insignificant from a fatigue damage standpoint and may be neglected. Hence, for off-resonance stresses of reasonable amplitude, accurate solutions may be obtained by truncating the series after nine terms, which involves all symmetric modes up to and including the 5-5. (e.g., 1-1, 1-3, 1-5, 3-1, ..., 5-3, 5-5)

Clamped Panel

To define the motion of the clamped panel, assume that the displacement consists of a series of comparison functions which satisfy all the boundary conditions (15). Functions which satisfy these requirements are the clamped beam mode functions given by Young and Felgar[18]. Hence, the panel displacement is of the form (11), or

$$W(X,Y;T) = \sum_{m=1}^{\infty} \sum_{n=1}^{\infty} A_{mn} W_{mn}(X,Y)\, e^{i\omega T} \tag{31}$$

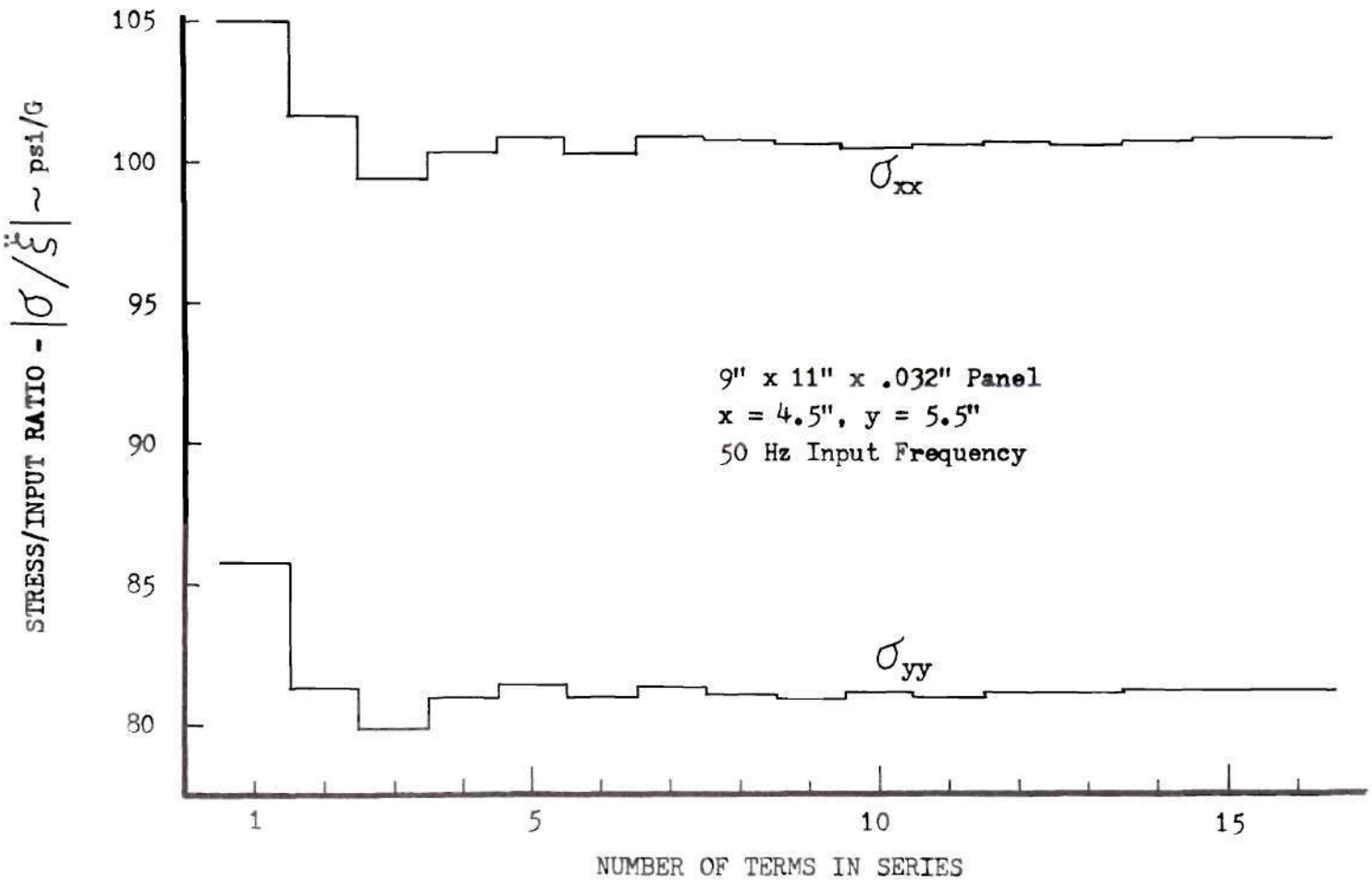

Figure 3. Convergence of Stress Functions, Simply Supported Panel, 50 Hz

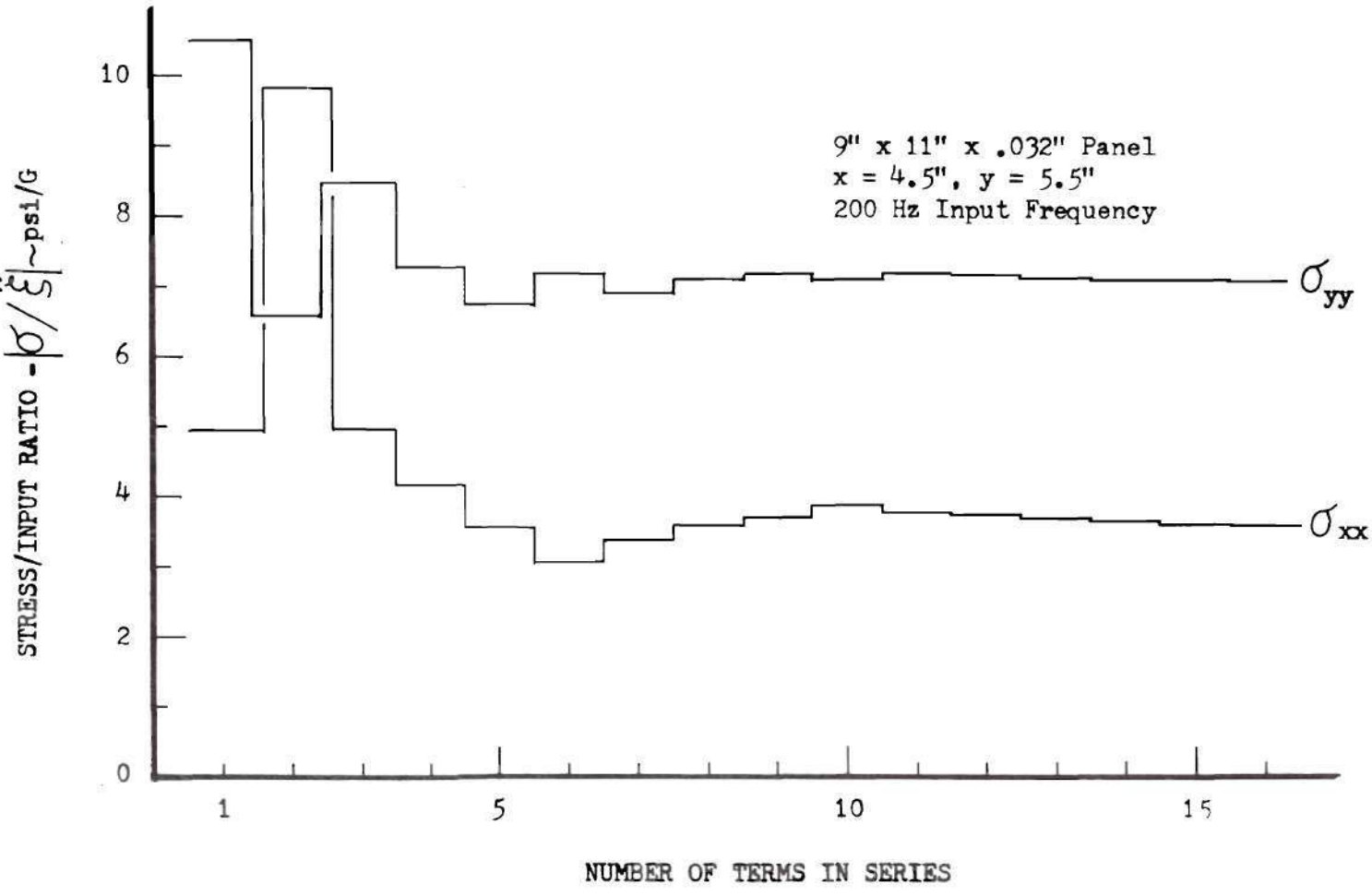

Figure 4. Convergence of Stress Functions, Simply Supported Panel, 200 Hz

where A_{mn} for this case is complex and includes the phase angle. The eigenfunctions W_{mn} are a combination of the clamped beam mode shapes

$$W_{mn}(x,y) = \phi_m(x)\,\psi_n(y) \tag{32}$$

where

$$\begin{aligned}\phi_m(x) &= \cosh\beta_m x - \cos\beta_m x - \alpha_m[\sinh\beta_m x - \sin\beta_m x]\\ \psi_n(y) &= \cosh\gamma_n y - \cos\gamma_n y - \theta_n[\sinh\gamma_n y - \sin\gamma_n y]\end{aligned} \tag{33}$$

The functions $\phi_m(x)$ and $\psi_n(y)$ are continuous on the interval $(0\leq x\leq a;\ 0\leq y\leq b)$; and since they are eigenfunctions resulting from the clamped beam eigenvalue equation, they satisfy the requirements for a complete set as defined by Courant and Hilbert[19]. The displacement (31) is then uniformly convergent in the panel domain. The completeness of the first and second derivatives has not previously been demonstrated; however, several authors, including Ballentine, et al[14] and Scruggs[20], have based their analyses on use of the completeness of the first derivatives.

The beam functions are solutions of the fourth-order differential equations

$$\phi_{m_{xxxx}} = \beta_m^4\,\phi_m \quad ; \quad \psi_{n_{yyyy}} = \gamma_n^4\,\psi_n \tag{34}$$

The values of the parameters $(\beta_m a)$ and $(\gamma_n b)$ are determined from the characteristic equations

$$\cos \beta_m a \cosh \beta_m a = 1$$

$$\cos \gamma_n b \cosh \gamma_n b = 1$$

The constants α_m and θ_n are evaluated from the equations

$$\alpha_m = \frac{\cosh \beta_m a - \cos \beta_m a}{\sinh \beta_m a - \sin \beta_m a}$$

$$\theta_n = \frac{\cosh \gamma_n b - \cos \gamma_n b}{\sinh \gamma_n b - \sin \gamma_n b}$$

Values of the above parameters, obtained from Reference (18) as functions of m and n, are summarized in Table 1.

The orthogonality relation (23) applied to the beam functions gives

$$\int_0^a \int_0^b \phi_m \phi_r \psi_n \psi_s \, dX dY = a b \delta_{mr} \delta_{ns} \tag{35}$$

The forced response of the panel is governed by equation (10), and upon substituting the displacements (9) and (31), and taking advantage of the differential relations (34) this equation yields

$$\sum_m \sum_n A_{mn} \left| \beta_m^4 \phi_m \psi_n + 2 \phi_{m_{XX}} \psi_{n_{YY}} + \gamma_n^4 \phi_m \psi_n - \lambda^4 \phi_m \psi_n \right| = \frac{\rho h \xi_0 \omega^2}{D}$$

Table 1. Parameters Used in Clamped Panel Stress Calculation

m,n	$(\beta_m a)$	α_m	$(\gamma_n b)$	θ_n
1	4.7300	0.9825	4.7300	0.9825
2	7.8532	1.0008	7.8532	1.0008
3	10.9956	0.9999	10.9956	0.9999
4	14.1372	1.0000	14.1372	1.0000
5	17.2788	↕	17.2788	↕
6	$(2m+1)\pi/2$		$(2n+1)\pi/2$	
↕	↕		↕	
m,n	$(2m+1)\pi/2$	1.0000	$(2n+1)\pi/2$	1.0000

Denote the second differentials by

$$U_{m(X)} = \phi_{m_{XX}} / \beta_m^2 \quad ; \quad V_{n(Y)} = \psi_{n_{YY}} / \gamma_n^2$$

Sybstitute these expressions into the preceding equation, multiply both sides by $\phi_r \psi_s$ and then integrate over the domain, recalling the orthogonality condition (35). This gives

$$\sum_m \sum_n \left[A_{mn} \left(\beta_m^4 + \gamma_n^4 - \lambda^4 \right) ab + 2 \sum_r \sum_s A_{rs} \beta_r^2 \gamma_s^2 K_{mr} K_{ns} ab \right] = \frac{\rho h \xi_o \omega^2}{D} \sum_m \sum_n \int_0^a \int_0^b \phi_m \psi_n \, dX dY \tag{36}$$

when m, n and r, s are odd. The above expression has been simplified by introduction of the parameters

$$K_{mr} = \frac{1}{a} \int_0^a U_m \phi_r \, dX \quad ; \quad K_{ns} = \frac{1}{b} \int_0^b V_n \psi_s \, dY$$

which are dimensionless quantities independent of the panel dimensions. These parameters and the integral on the right side of equation (36) may be evaluated with the aid of the integration tables in Reference (21). Hence,

$$K_{mr} = \frac{8(\beta_r a)^2(\alpha_r \beta_r a - \alpha_m \beta_m a)}{(\beta_r a)^4 - (\beta_m a)^4} \qquad \text{(m, r odd)}$$

$$K_{mm} = (\alpha_m/\beta_m a)(2 - \alpha_m \beta_m a) \qquad \text{(m odd)} \tag{37}$$

$$K_{ns} = \frac{8(\gamma_s b)^2(\theta_s \gamma_s b - \theta_n \gamma_n b)}{(\gamma_s b)^4 - (\gamma_n b)^4} \qquad \text{(n, s odd)}$$

$$K_{nn} = (\theta_n/\gamma_n b)(2 - \theta_n \gamma_n b) \qquad \text{(n odd)} \tag{38}$$

Upon evaluating the integral in equation (36) the infinite system of equations

$$A_{mn}(\beta_m^4 + \gamma_n^4 - \lambda^4) + 2\sum_{r}^{\text{odd}}\sum_{s} A_{rs}\beta_r^2\gamma_s^2 K_{mr}K_{ns} = \frac{16\rho h \xi_o \omega^2}{D}\left(\frac{\alpha_m \theta_n}{\beta_m a \gamma_n b}\right) \tag{39}$$

are established, from which the values of A_{mn} can be determined.

Manipulation of the preceding infinite set of equations is greatly simplified by rewriting the equations in matrix form. In view of the good convergence of the system (39), and due to practical limitations in solving the set of equations, the series is truncated after a finite number of terms.

Denote

$$[D] = \left[(\beta_m^4 + \gamma_n^4)[I] + 2(\beta_r^2\gamma_s^2 K_{mr}K_{ns})\right]$$

$$\{P\} = \frac{16\rho h \xi_o \omega^2}{D}\left\{\frac{\alpha_m \theta_n}{\beta_m a \gamma_n b}\right\} = \frac{16\rho h \ddot{\xi}}{D}\left\{\frac{\alpha_m \theta_n}{\beta_m a \gamma_n b}\right\}$$

The matrix $\left[D\right]$ is a pseudo-dynamical matrix similar to the dynamical matrix in discrete systems. The matrix $\left[I\right]$ is the identity matrix. The truncated set of equations (39) may then be written in the convenient form

$$\left[\left[D\right] - \lambda^4\left[I\right]\right]\left\{A\right\} = \left\{P\right\} \tag{40}$$

Natural Frequencies

The natural frequencies of the clamped panel are determined by equating the determinant of the coefficients of $\left\{A\right\}$ to zero when $\left\{P\right\}$ is zero. Replacing λ^4 by the eigenvalue η_{mn}^4 corresponding to the free vibration, the characteristic equation

$$\left|\left[D\right] - \eta_{mn}^4\left[I\right]\right| = 0$$

is obtained. The roots of this equation are

$$\eta_{11}\ ,\ \eta_{13}\ ,\ \eta_{31}\ ,\ \eta_{33}\ ,\cdots,\eta_{NN}$$

The damped natural frequencies are then obtained by combining expressions (8), (17) and (18) to yield the familiar expression

$$\Omega_{mn} = \omega_{mn}\sqrt{1 - \zeta^2} \tag{41}$$

where

$$\omega_{mn} = \eta_{mn}^2 \sqrt{\frac{D}{\rho h}} \tag{42}$$

are the undamped natural frequencies.

Forced Vibration

The steady-state forced response of the clamped panel is obtained from equation (40). First let

$$[Z] = \left[[D] - \lambda^4 [I]\right]$$

where λ^4 is defined by equation (13) and is a function of the forcing frequency. The modal column $\{A\}$ corresponding to a given value of the forcing frequency is determined by premultiplying equation (40) by the inverse of the $[Z]$ matrix to give

$$\{A\} = [Z]^{-1}\{P\} \tag{43}$$

The displacement of the clamped panel, stated previously as the infinite series (31), can now be written in matrix form, for a given frequency, by taking the transpose of $\{A\}$.

$$W = \{A\}^T\{W\}e^{i\omega T} = \lfloor A \rfloor \{W\}e^{i\omega T} \tag{44}$$

where $\{W\}$ is the matrix of the eigenfunctions W_{mn}. The deflection series has been truncated at N terms to obtain the above solutions.

Dynamic Stresses

The dynamic stress relations given by equation (28) also apply for the clamped panel. These expressions may be written in matrix notation and upon substitution of the displacement w, yield

$$\sigma_{X\text{-}X} = \frac{E z}{1-\nu^2} \lfloor A \rfloor \{ \phi_{m_{XX}} \psi_n + \nu \phi_m \psi_{n_{YY}} \}$$

$$\sigma_{Y\text{-}Y} = \frac{E z}{1-\nu^2} \lfloor A \rfloor \{ \phi_m \psi_{n_{YY}} + \nu \phi_{m_{XX}} \psi_n \}$$

Introducing the previously defined parameters $U_m(x)$ and $V_n(y)$, and again noting that the maximum stresses occur at the panel surface, the stress equations

$$\sigma_{X\text{-}X} = \lfloor A \rfloor \{ M_{X\text{-}X} \} e^{i\omega T} \quad ; \quad \sigma_{Y\text{-}Y} = \lfloor A \rfloor \{ M_{Y\text{-}Y} \} e^{i\omega T} \tag{45}$$

are obtained, where

$$\{M_{X\text{-}X}\} = \frac{E h}{2[1-\nu^2]} \{ \beta_m^2 U_m \psi_n + \nu \gamma_n^2 \phi_m V_n \}$$

$$\{M_{Y\text{-}Y}\} = \frac{E h}{2[1-\nu^2]} \{ \gamma_n^2 \phi_m V_n + \nu \beta_m^2 U_m \psi_n \} \tag{46}$$

are column matrices of order N x 1.

The above expressions determine the dynamic stresses at any point (x,y) in the clamped panel under the action of a sinusoidal boundary displacement. The influence of the boundary acceleration and the forcing frequency are included in the transposed modal matrix $\{A\}^T$. As mentioned previously, this is a 1 x N complex matrix.

Since the mode functions chosen for this analysis are not exact solutions to the differential equations of motion for the clamped plate, there will be significant coupling between the modes. The rate of convergence of the natural frequencies and dynamic stresses was investigated by varying the size of the truncated series. The natural frequencies for the first four modes are compared below for values of N = 4, 9 and 16.

	MODE			
N	1-1	1-3	3-1	3-3
4	114.7	350.7	483.5	700.9
9	114.7	350.4	483.1	698.0
16	114.7	350.3	483.0	697.1

As noted, the four-term solution yields a natural frequency within .55% of the 16 term series for the 3-3 mode, while there is no difference in the first mode. The above natural frequencies are approaching the exact value from above as the size of the series increases.

Convergence of the stress functions was checked at frequencies of 50 and 200 Hz and at the first four natural frequencies. The results of these calculations are shown in Figures 5, 6, and 7. The maximum

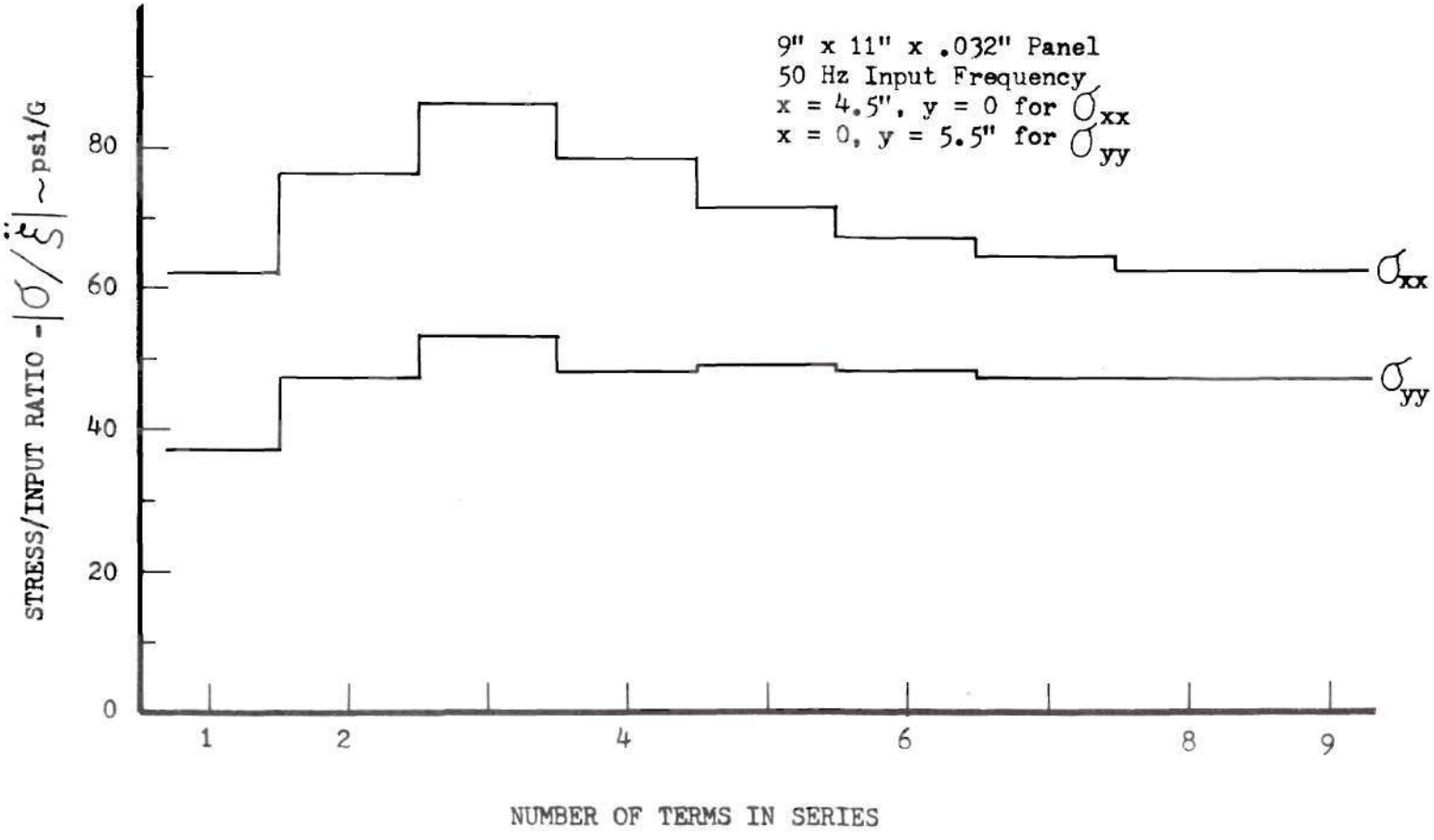

Figure 5. Convergence of Stress Functions, Clamped Panel, 50 Hz

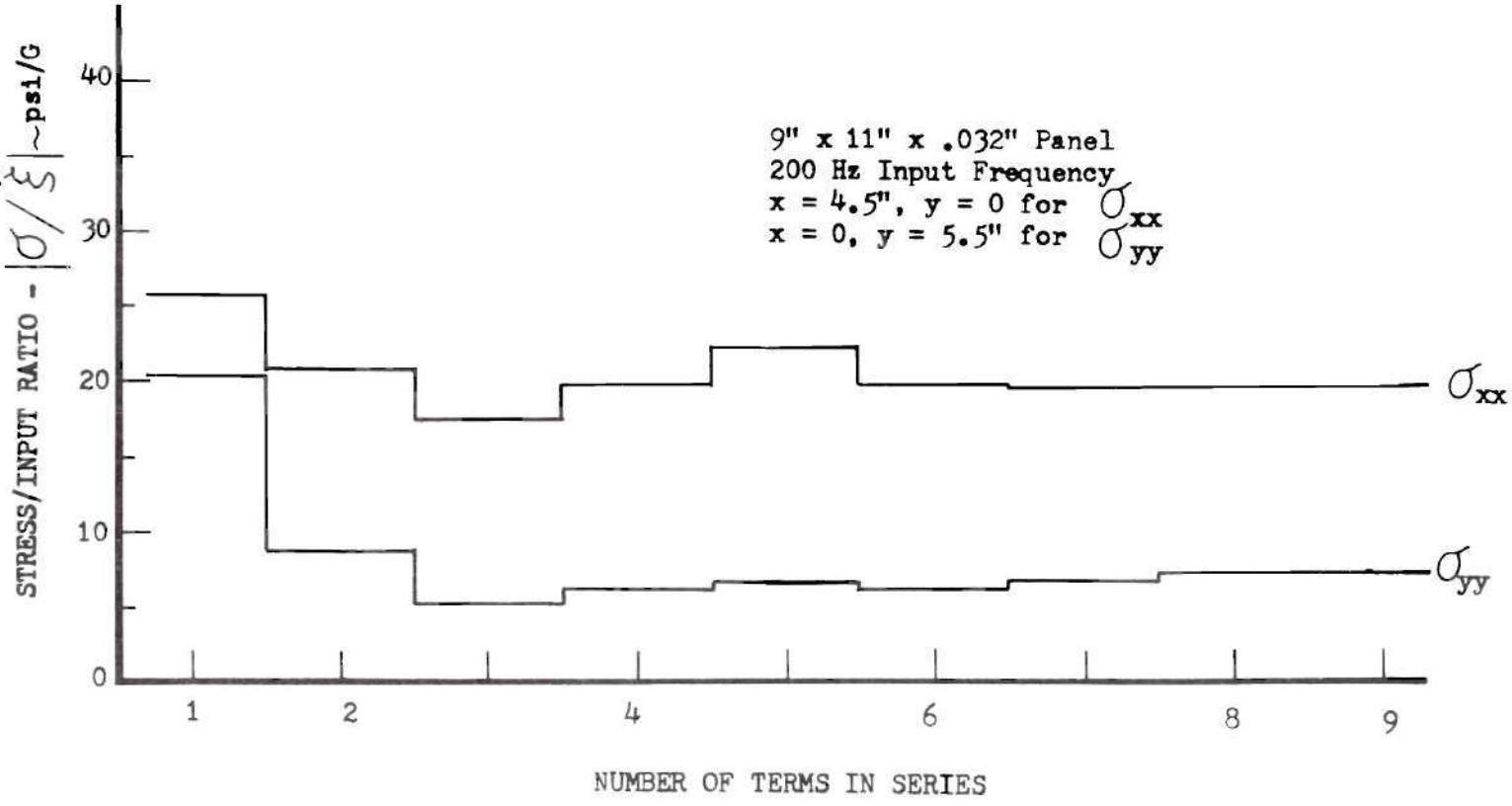

Figure 6. Convergence of Stress Functions, Clamped Panel, 200 Hz

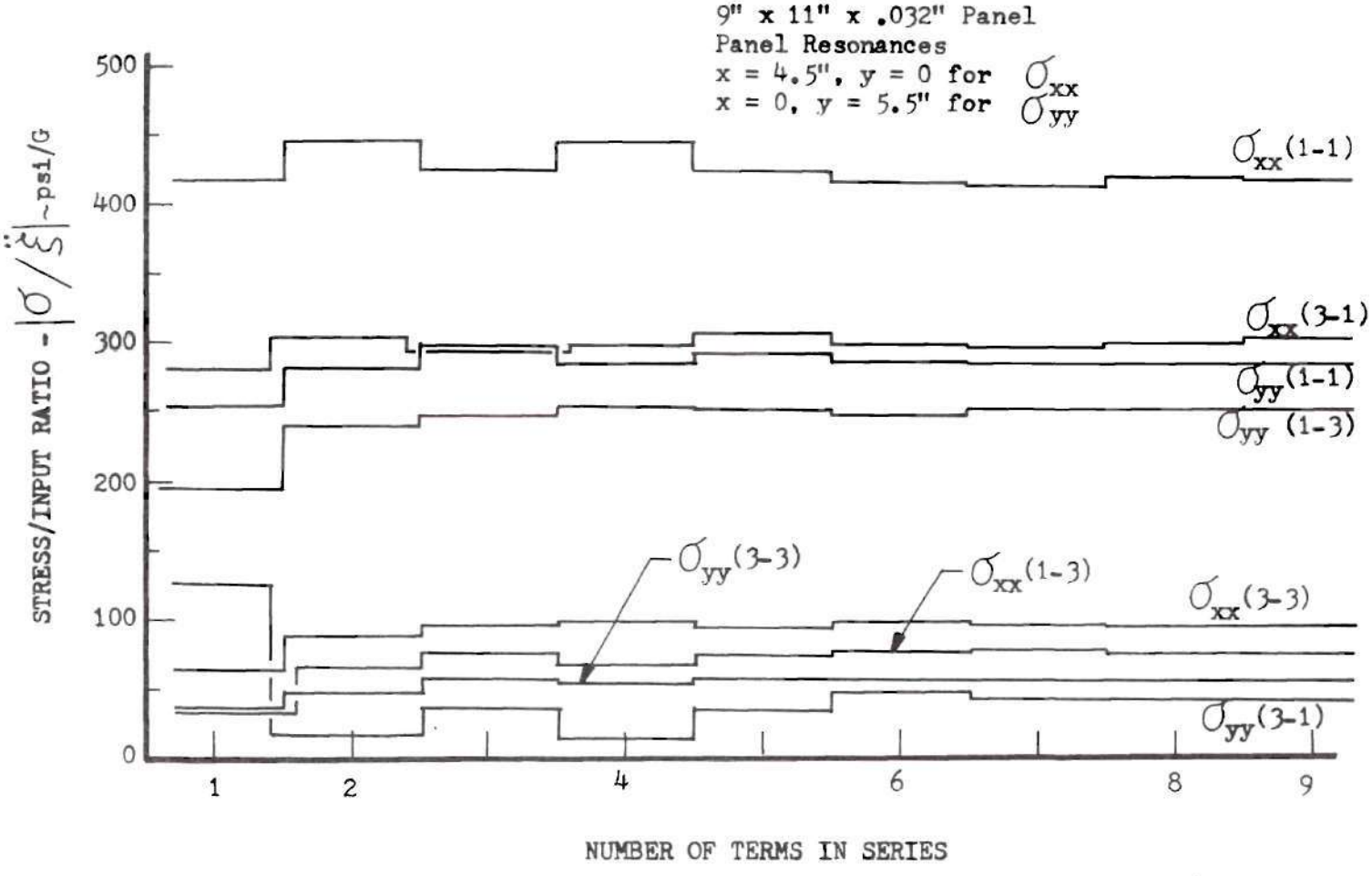

Figure 7. Convergence of Stress Functions, Clamped Panel, Resonance

variation noted for the off-resonance stresses is approximately 200% of the value at the end of nine terms. However, the principal concern is with the resonant stress, particularily for the first four modes. As noted in Figure 7, a few of the modal stresses undergo considerable variation in the first two or three terms. The higher stresses, which are the most important from a fatigue damage viewpoint, occur in the fundamental mode and exhibit less variation. The variation in the x-direction stress for the first mode is less than 7%, which is within normal experimental accuracy. Although there is still a certain degree of variation after nine terms in the series, which includes all modes up to the 5-5, the stresses appear to be approaching limiting values. However, no definite conclusions can be made regarding absolute convergence of the stress functions.

Computer Programs

Programming the analytical results for rapid solution comprised an integral part of the analysis effort. The simply supported and clamped panel analyses were programmed on the Lockheed-Georgia Company remote access computer. The results presented for the convergence analysis were obtained from these programs. A parameter study was conducted using these programs and the results are presented in Appendix I. Typical outputs from these programs are included in Appendix II using the test specimen parameters.

Programming of the simply supported analysis posed no major problems. However, due to the complexity of the clamped panel analysis, it became necessary to limit the number of terms in the expansion to

four for most operations. The basic program was set up to truncate the series only at m = n terms. Hence, the possibilities to be considered were matrices of 4 by 4 (up to the 3-3 mode), 9 by 9 (up to the 5-5 mode), 16 by 16 (up to the 7-7 mode), etc. A complex matrix inversion subroutine used with the main program proved to be the limiting factor, as the process involved in inverting a 16 by 16 matrix, operating in conjunction with the main program, exceeded the capacity of the remote access computer. The 9 by 9 matrix inversion was possible but required more machine time to accomplish than the 4 by 4 matrix inversion. For these reasons, the results presented in the following chapters and Appendix I were obtained using only a four-term solution (4 by 4 matrix). Since the analytical results were modified by comparison with the measured data (See Chapter IV), the error induced by this simplification should be within the experimental error.

CHAPTER III

EXPERIMENTAL PROCEDURE

A vibration test was conducted on a typical structural panel in the Acoustics Laboratory of the Aeromechanics Division of the Lockheed-Georgia Company. The objective of this program was to obtain data to either substantiate or modify the stress relationships derived in Chapter II. Dynamic stresses in a flat aluminum panel were measured under vibratory loading using both the simply supported and clamped edge fixities discussed previously.

Similar unpublished experiments conducted in conjunction with Reference 22 defined one potential problem area which could drastically affect the test data. The tests were conducted to determine the edge fixity requirements for a clamped panel. The frame thickness was gradually increased and made more rigid while simultaneously decreasing the panel rigidity. However, as the panel rigidity decreased, small variations in room temperature caused expansion or contraction of the thin panel while the massive frame was virtually unaffected. Under controlled conditions a $4^{\circ}F$ increase in temperature caused a 50% reduction in the fundamental mode frequency. The test panel in this instance was 0.020" aluminum while the frame was $\frac{1}{2}$" steel.

In an effort to minimize the temperature effects on the natural frequencies and dynamic stresses the frames were fabricated of aluminum, giving the same coefficient of expansion for both test panel and frame.

Additionally, although the room temperature could not be controlled exactly due to the presence of the shaker amplifier in the room, data were taken only after the shaker and amplifier had been running for approximately 30 minutes, at which time the room temperature stabilized.

Test Specimen

The test specimen selected was a 2024-T6 aluminum panel, 0.032" thick, with surface dimensions of 11" by 13". Two different aluminum frames were fabricated to attain the simply supported and clamped edge conditions, with the same test panel being used in both frames. Details of these frames are shown in Figures 8 and 9. The effective panel (unrestrained) dimensions in both frames were a = 9" and b = 11".

The panel was restrained in the simply supported frame by pressure between the wedges and was therefore restricted from in-plane motion at the boundaries, which represents a departure from idealized boundary conditions. This type of attachment was selected as a compromise of the ideal condition which would require extensive machining of the frame and panel and would be quite sensitive to vibration. The clamped panel was constrained by the bolts through the frame and panel and, to achieve uniform edge clamping around the boundary, the bolts were torqued to 25 inch-pounds prior to testing.

Test Setup

The test specimen, installed in the appropriate frame, was mounted on an MB Electronics C-10E 1200-pound-force shaker so that uniform lateral motion was applied to the frame, as shown in Figure 10.

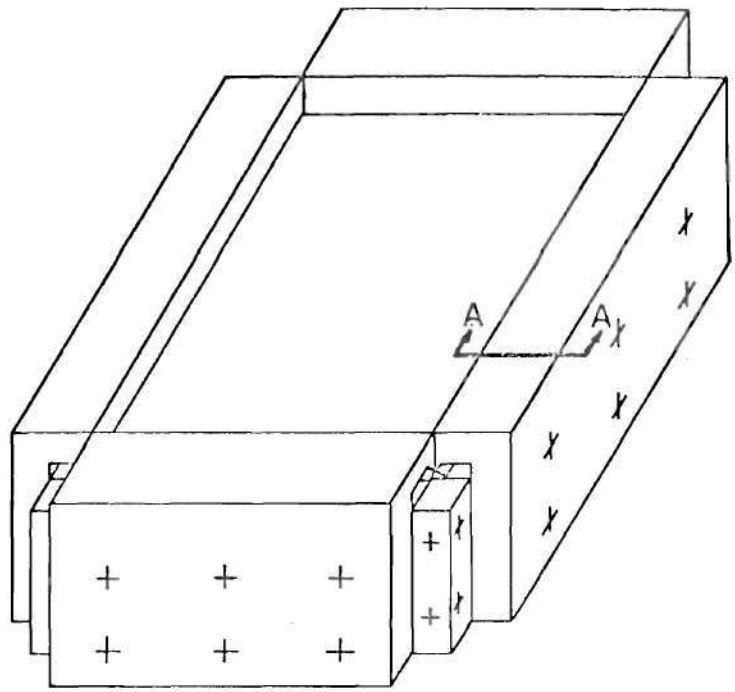

END VIEW OF FRAME

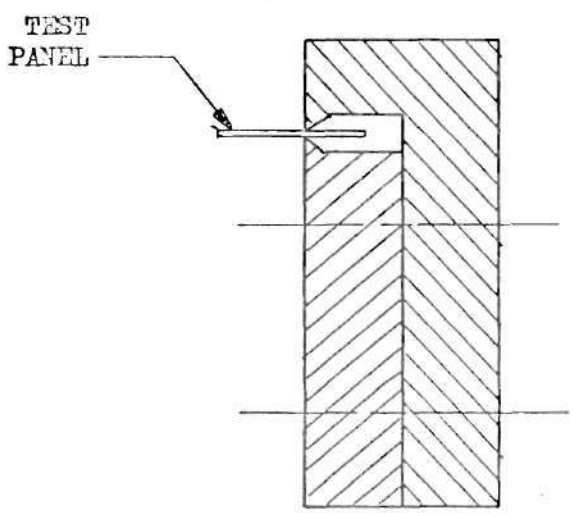

SECTION A-A

Figure 8. Simply Supported Panel Frame

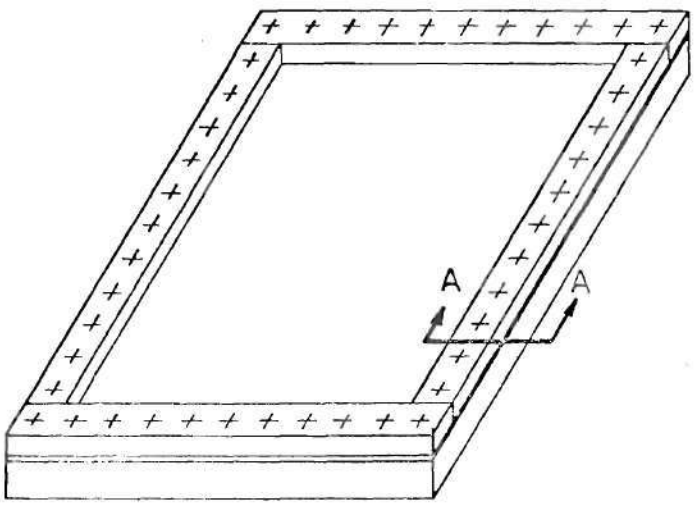

END VIEW OF FRAME

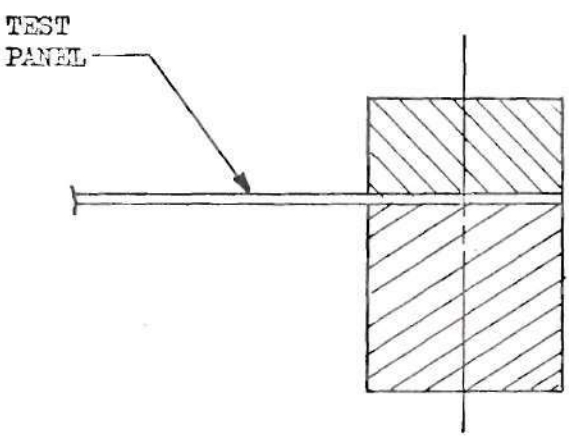

SECTION A-A

Figure 9. Clamped Panel Frame

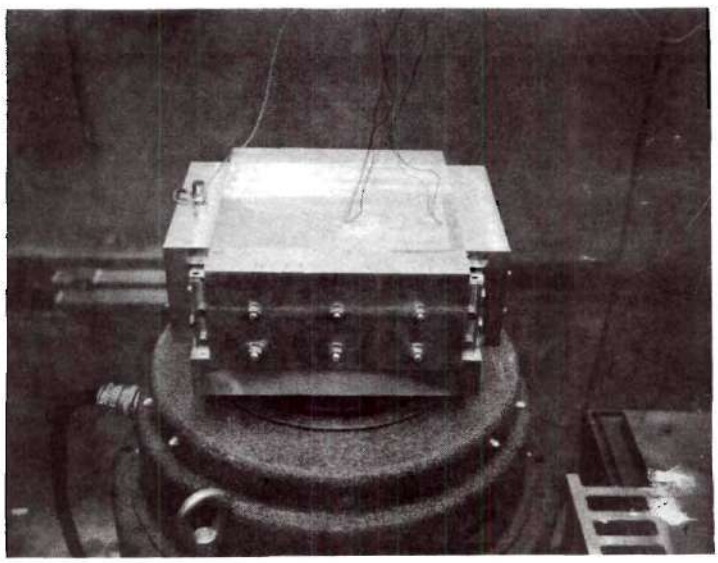

SIMPLY SUPPORTED PANEL

CLAMPED PANEL

Figure 10. Test Specimen Installed on Shaker

An accelerometer was mounted on each end of the frame to monitor and control the shaker output.

The equipment setup is shown diagrammatically in Figure 11. As shown in the diagram, the accelerometer output formed a closed loop system to maintain a constant input acceleration level over the desired frequency range. The strain gage output (voltage change) was passed through a signal conditioner which provided the balance resistance and excitation voltage for the strain gage. After being amplified, the signal was filtered through a dynamic analyzer using a 2 Hz filter to obtain only the stress component at the exciting frequency. The filtered signal was then plotted versus frequency to obtain the spectrum plot.

Test Procedure

A modal survey was conducted with the panel in the clamped frame to determine optimum locations for the strain gages. The first 16 uncoupled modes were located by their Chladni patterns and node lines were marked on the panel. The results of this survey were used to locate the 15 uni-axial strain gages for measuring dynamic strain. Detailed strain gage locations and orientations are shown in Figure 12.

Frequency Sweeps

With the strain gages installed, frequency sweeps were made on both panels at the following constant input acceleration levels:

$$0.4,\ 0.6,\ 0.8,\ 1.0,\ 1.5,\ 2.0,\ 2.5,\ 3.0\ G_{rms}$$

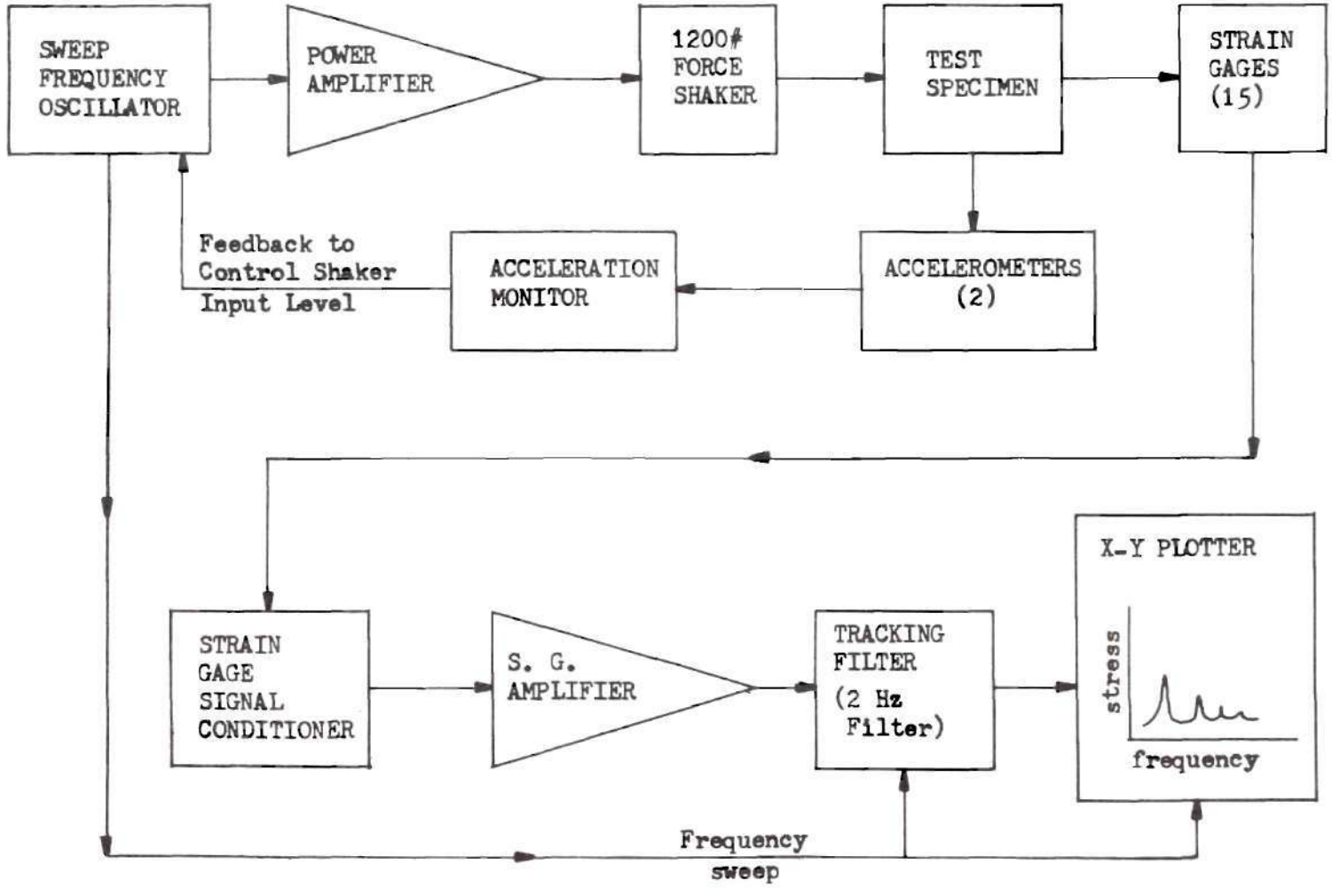

Figure 11. Test Equipment Schematic Diagram

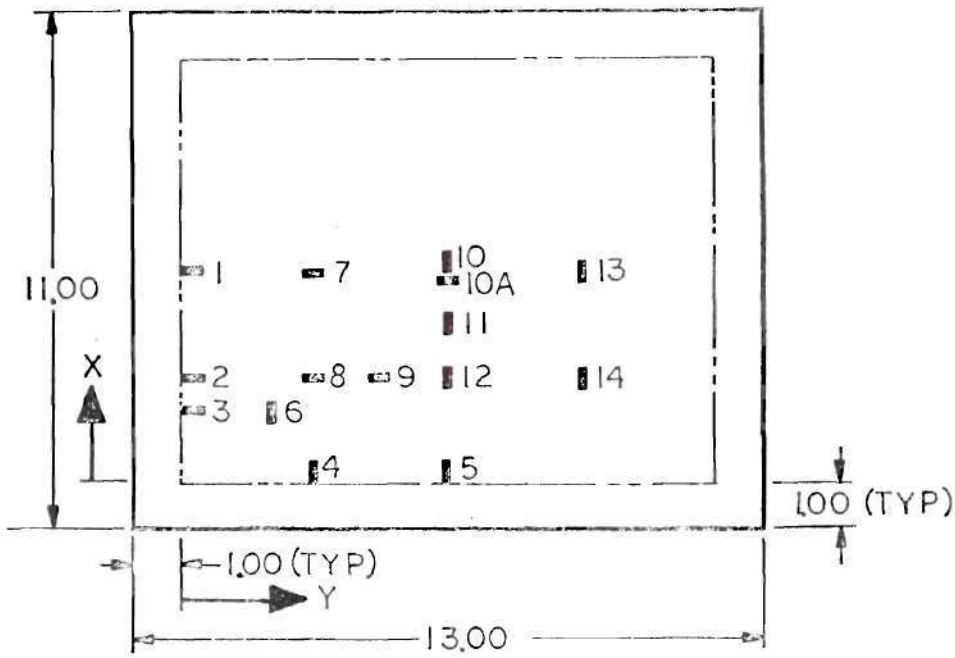

COORDINATES OF STRAIN GAGES		
STRAIN GAGE NO.	X	Y
1	a/2	0
2	a/4	0
3	a/6	0
4	0	b/4
5	0	b/2
6	a/6	b/6
7	a/2	b/4
8	a/4	b/4
9	a/4	3b/8
10	a/2	b/2
10A	a/2	b/2
11	3a/8	b/2
12	a/4	b/2
13	a/2	3b/4
14	a/4	3b/4

Figure 12. Strain Gage Locations

The input level was controlled automatically by the accelerometer feedback, as discussed previously. Stress versus frequency plots were recorded from 20 to 1000 Hz for each of the 15 strain gages at each of the above input acceleration levels.

Test Results

Natural frequencies for the test panels were determined from the spectrum plots and are shown in Table 2 compared with the calculated values. All modes but the first show good agreement.

Typical stress response curves are shown in Figures 13 and 14 for strain gages 10 and 10A, respectively, on the simply supported panel. These gages are located at the center of the panel and show the maximum stress. Figures 15 and 16 show the stress response curves for strain gages 1 and 5 respectively, on the clamped panel. These gages are located at the mid-point of the edges and again show the maximum stress excursions. Several of the antisymmetric modes were also excited during the frequency sweeps; however, since these modes were not coupled with the symmetric modes, their presence did not affect the desired date. The existence of the antisymmetric modes under uniform loading conditions is attributed to an unbalance of the specimen created by a combination of the installation of the strain gages and uneven distribution of the panel/frame weight on the shaker head.

Summaries of all stress levels for the first four symmetrical modes are given in Tables 3 and 4 for the simply supported and clamped panels, respectively. Detailed discussion of these data will be delayed until the following chapter, since the primary purpose of the data will be to verify the analytical results.

Table 2. Comparison of Calculated and Measured Natural Frequencies

m \ n	1	2	3
1	f_c = 62 f_m = 35	f_c = 137 f_m = 151	f_c = 262 f_m = 281
2	f_c = 174 f_m = 187	f_c = 245 f_m = 203	f_c = 373 f_m = 387
3	f_c = 360 f_m = 353	f_c = 435 f_m = 443	f_c = 560 f_m = 561

SIMPLY-SUPPORTED PANEL

m \ n	1	2	3
1	f_c = 115 f_m = 58	f_c = 206 f_m = 200	f_c = 351 f_m = 354
2	f_c = 262 f_m = ---	f_c = 345 f_m = 323	f_c = 485 f_m = ---
3	f_c = 483 f_m = 458	f_c = 566 f_m = 523	f_c = 701 f_m = 655

CLAMPED PANEL

f_c Calculated frequency ~ Hz

f_m Measured frequency ~ Hz

m 9 inch dimension

n 11 inch dimension

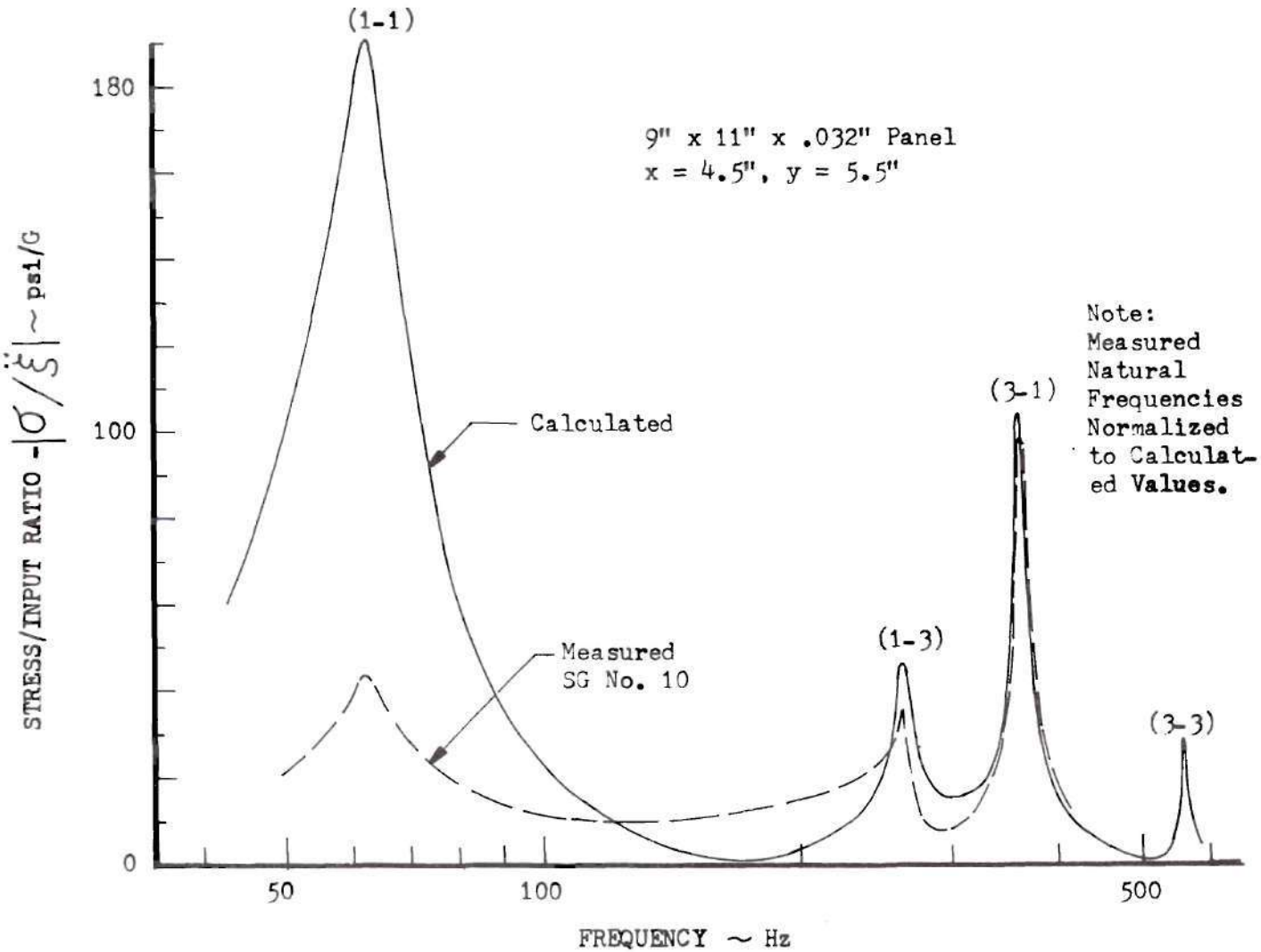

Figure 13. Comparison of Calculated and Measured Stress Response, Simply Supported Panel, SG 10

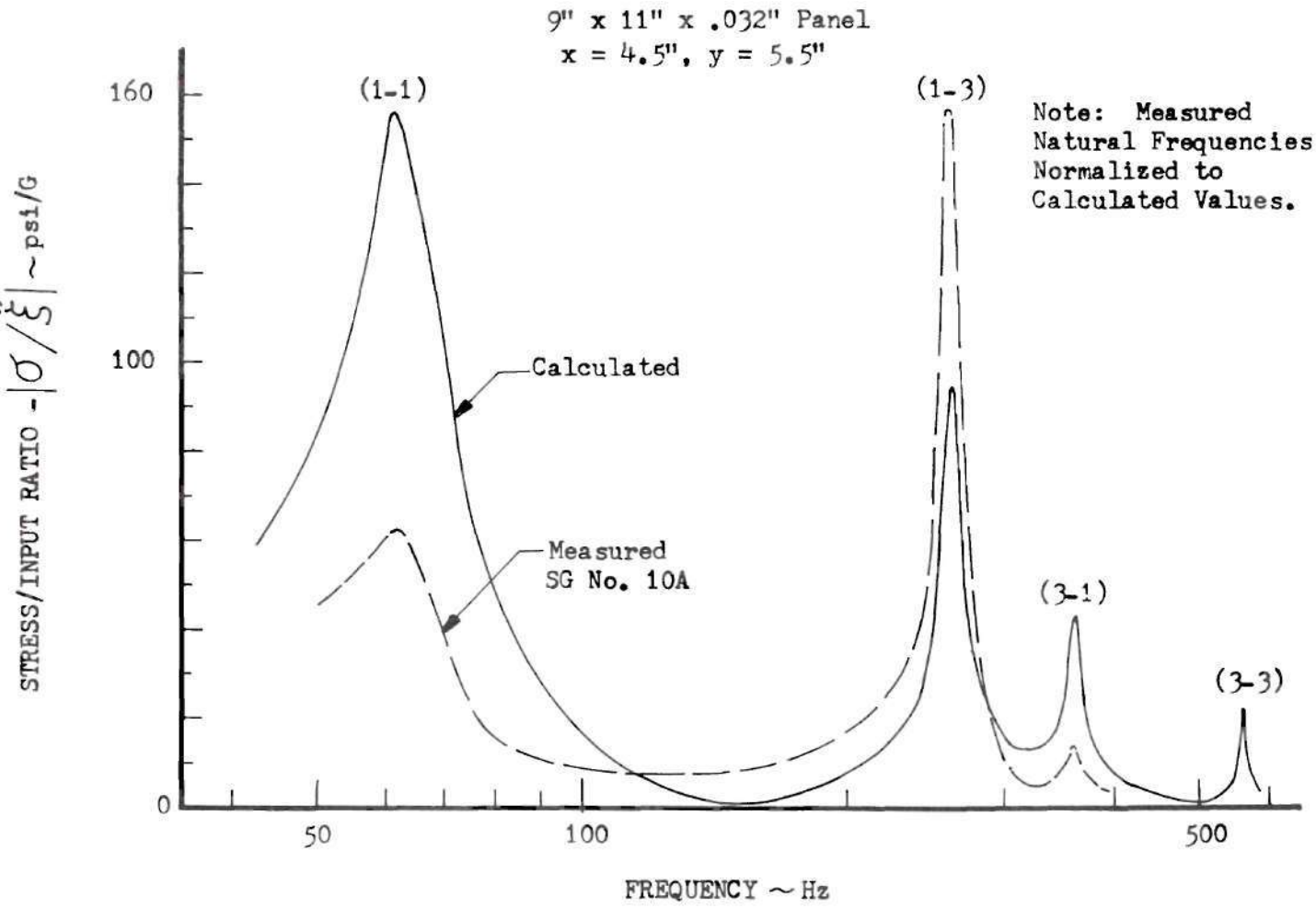

Figure 14. Comparison of Calculated and Measured Stress Response, Simply Suported Panel, SG 10A

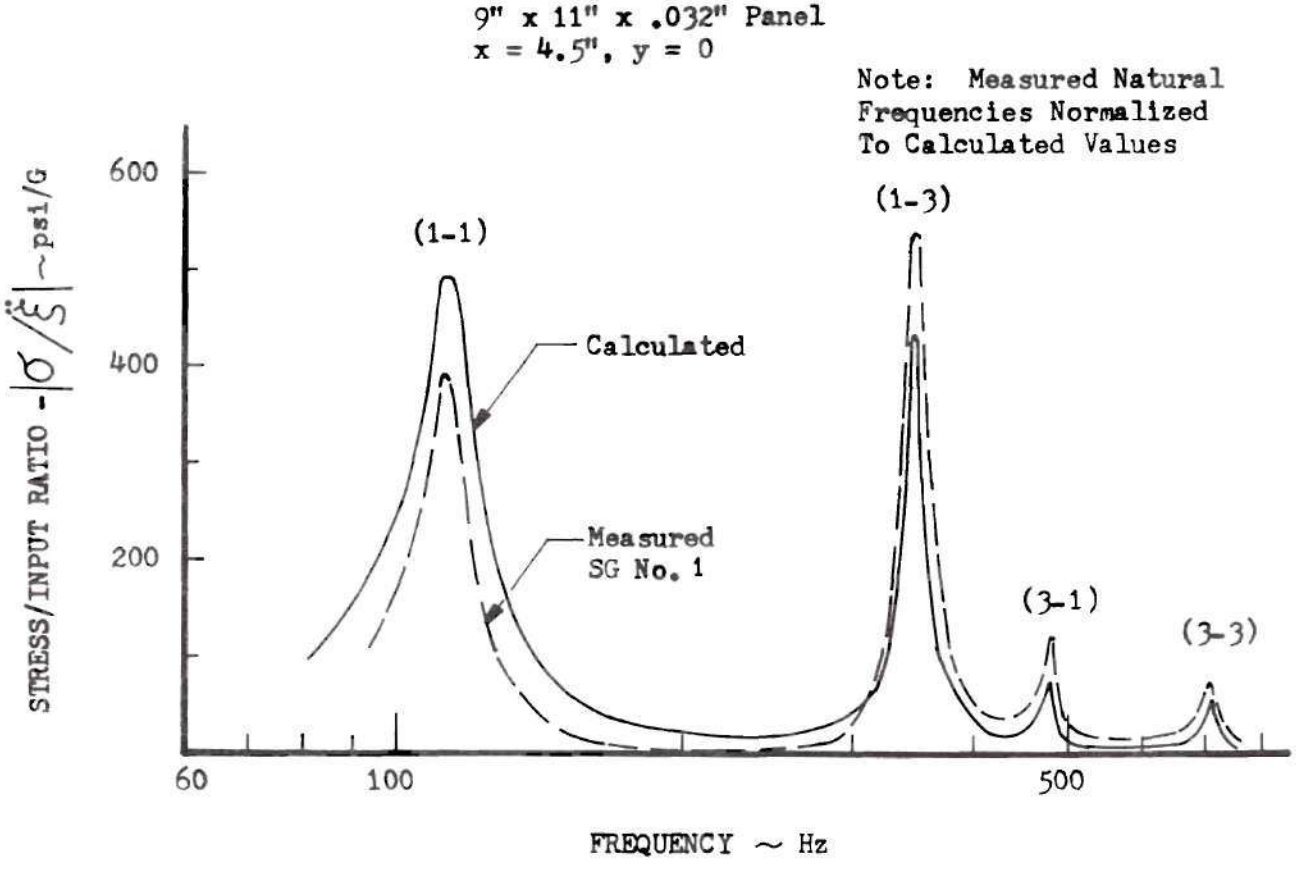

Figure 15. Comparison of Calculated and Measured Stress Response, Clamped Panel, SG 1

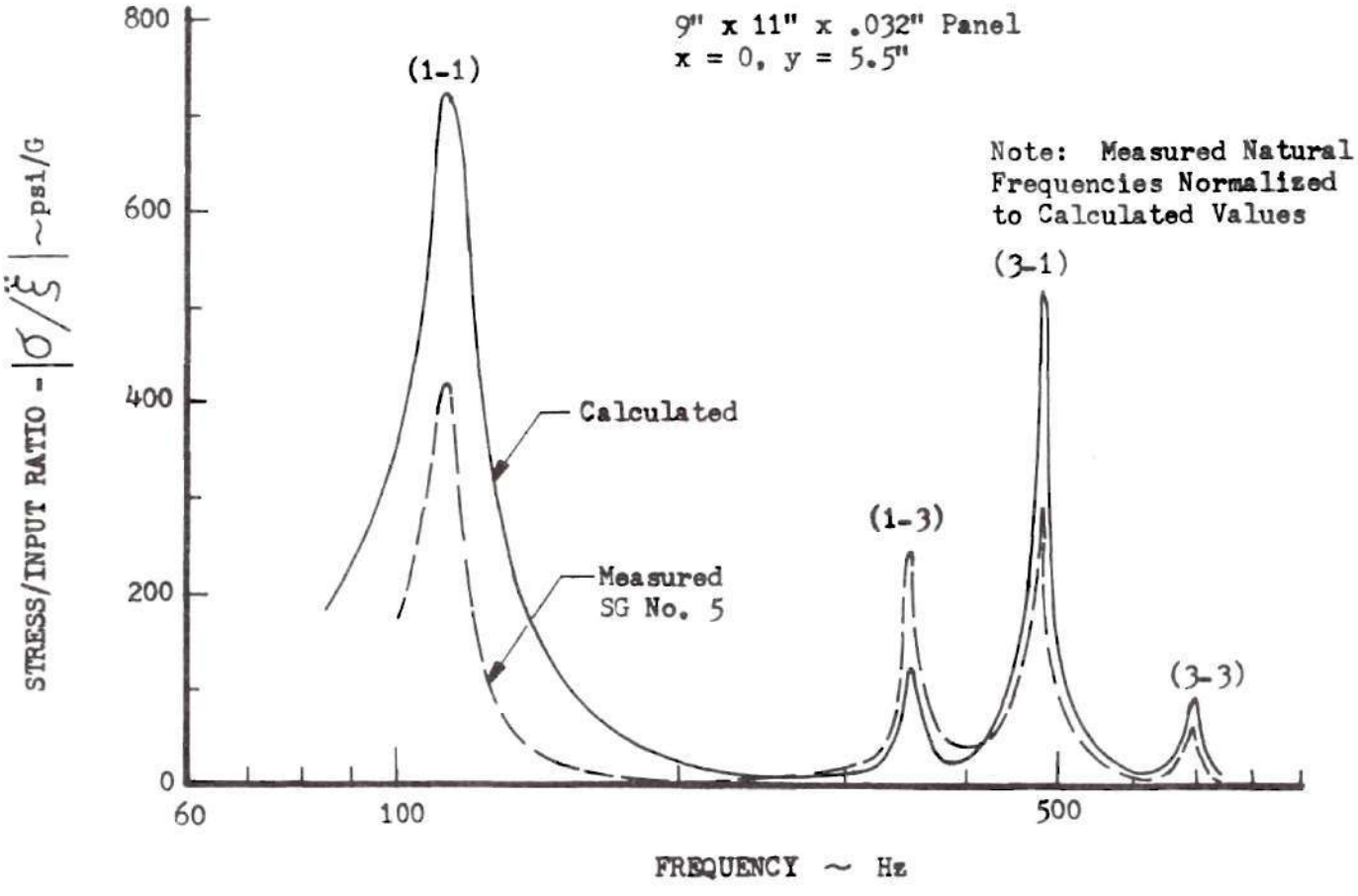

Figure 16. Comparison of Calculated and Measured Stress Response, Clamped Panel, SG 5

Table 3. Summary of Test Results, Simply Supported Panel

ξ	SG No. 1 (x = a/2, y = 0)				SG No. 2 (x = a/4, y = 0)			
	MODE NO.				MODE NO.			
	1-1	1-3	3-1	3-3	1-1	1-3	3-1	3-3
.4	10	5	3	-	7	-	2	-
.6	18	12	6	-	-	-	-	-
.8	22	16	10	-	-	-	-	-
1.0	25	27	10	-	20	16	10	-
1.5	35	52	17	-	-	-	-	-
2.0	42	72	24	-	30	37	18	-
2.5	50	90	31	-	35	52	25	-
ξ	SG No. 4 (x = 0, y = b/4)				SG No. 5 (x = 0, y = b/2)			
	MODE NO.				MODE NO.			
	1-1	1-3	3-1	3-3	1-1	1-3	3-1	3-3
.4	20	10	6	-	25	12	6	-
.6	34	16	12	-	40	21	10	-
.8	48	22	15	-	55	29	15	-
1.0	52	24	14	-	65	36	18	-
1.5	72	37	20	-	86	54	28	-
2.0	91	49	25	-	104	68	34	-
2.5	104	65	32	-	123	86	39	-
ξ	SG NO. 6 (x = a/6, y = b/6)				SG NO. 7 (x = a/2, y = b/4)			
	MODE NO.				MODE NO.			
	1-1	1-3	3-1	3-3	1-1	1-3	3-1	3-3
.4	10	4	15	5	6	37	-	-
.6	-	-	-	-	6	49	-	-
.8	-	-	-	-	12	70	-	5
1.0	30	8	38	15	20	87	-	20
1.5	42	19	60	26	44	134	-	32
2.0	56	27	78	34	56	176	-	40
2.5	65	34	100	45	72	232	-	58
ξ	SG NO. 8 (x = a/4, y = b/4)				SG NO. 9 (x = a/4, y = 3b/8)			
	MODE NO.				MODE NO.			
	1-1	1-3	3-1	3-3	1-1	1-3	3-1	3-3
.4	5	29	-	-	8	14	0	5
.6	15	49	-	-	17	24	3	6
.8	20	68	-	-	21	30	2	7
1.0	26	83	-	-	30	43	5	10
1.5	36	127	-	-	46	66	10	16
2.0	45	164	-	-	61	88	15	20
2.5	61	213	-	-	78	107	19	25

Note: Input acceleration levels are in G_{rms}. All stress levels are in psi_{rms}. The stress levels shown are the maximum values read during resonance.

Table 3. (Con't)

ξ	SG NO. 10 (x = a/2, y = b/2)				SG NO. 10A (x = a/2, y = b/2)			
	MODE NO.				MODE NO.			
	1-1	1-3	3-1	3-3	1-1	1-3	3-1	3-3
.4	26	11	35	-	27	62	3	-
.6	46	23	56	-	40	95	8	-
.8	61	30	76	-	52	125	11	-
1.0	80	38	96	-	61	158	13	-
1.5	113	59	142	-	91	249	20	-
2.0	133	73	190	-	124	320	30	-
2.5	144	94	239	-	149	412	37	-
ξ	SG NO. 11 (x = 3a/8, y = b/2)				SG NO. 12 (x = a/4, y = b/2)			
	MODE NO.				MODE NO.			
	1-1	1-3	3-1	3-3	1-1	1-3	3-1	3-3
.4	22	9	21	12	20	6	25	-
.6	39	11	29	17	25	10	34	-
.8	54	19	41	23	38	17	48	-
1.0	66	25	52	30	50	22	62	-
1.5	94	39	75	47	76	34	89	-
2.0	116	50	100	62	96	43	116	-
2.5	140	64	125	80	115	54	148	-
ξ	SG NO. 13 (x = a/2, y - 3b/y)				SG NO. 14 (x = a/4, y = 3b/4)			
	MODE NO.				MODE NO.			
	1-1	1-3	3-1	3-3	1-1	1-3	3-1	3-3
.4	13	7	26	-	11	4	22	-
.6	22	13	39	-	19	6	31	-
.8	29	17	53	-	30	9	40	-
1.0	35	24	65	-	39	11	52	-
1.5	51	35	94	-	60	18	79	-
2.0	69	48	129	-	78	23	99	-
2.5	84	65	154	-	91	32	120	-

Table 4. Summary of Test Results, Clamped Panel

$\sqrt{\frac{W}{g}}$	SG NO. 1 (x = a/2, y = 0)				SG NO. 2 (x = a/4, y = 0)			
	MODE NO.				MODE NO.			
	1-1	1-3	3-1	3-3	1-1	1-3	3-1	3-3
.4	222	215	47	25	127	126	91	20
.6	296	316	77	42	170	184	141	33
.8	348	417	101	56	205	253	196	50
1.0	399	546	131	72	231	323	261	58
1.5	504	825	180	97	295	531	421	87
2.0	595	1130	260	137	345	730	550	110
2.5	655	1450	300	160	385	930	680	120
3.0	-	1777	370	190	424	1180	760	150
$\sqrt{\frac{W}{g}}$	SG NO. 4 (x = 0, y = b/4)				SG NO. 5 (x = 0, y = b/2)			
	MODE NO.				MODE NO.			
	1-1	1-3	3-1	3-3	1-1	1-3	3-1	3-3
.4	187	80	179	20	230	89	106	23
.6	235	123	290	35	306	138	181	36
.8	283	172	403	50	370	190	230	50
1.0	316	220	500	57	419	242	293	60
1.5	401	350	790	83	542	392	426	88
2.0	475	470	1010	100	645	530	560	110
2.5	540	630	1230	120	-	700	650	133
3.0	-	800	1400	150	-	880	760	167
$\sqrt{\frac{W}{g}}$	SG NO. 6 (x = a/6, y = b/6)				SG NO. 7 (x = a/2, y = b/4)			
	MODE NO.				MODE NO.			
	1-1	1-3	3-1	3-3	1-1	1-3	3-1	3-3
.4	-	8	48	12	41	108	5	9
.6	-	10	83	20	55	160	10	13
.8	-	13	113	28	66	218	12	18
1.0	-	16	144	33	72	274	15	22
1.5	-	22	226	50	100	440	23	32
2.0	-	30	305	65	118	620	32	42
2.5	-	34	364	80	131	770	35	44
3.0	-	38	432	98	-	945	40	60

Note: Input acceleration levels are in G_{rms}. All stress levels are in psi_{rms}. The stress levels shown are the maximum values read during resonance.

Table 4. (Con't)

ξ	SG NO. 8 (x = a/4, y = b/4)				SG NO. 9 (x = a/4, y = 3b/8)			
	MODE NO.				MODE NO.			
	1-1	1-3	3-1	3-3	1-1	1-3	3-1	3-3
.4	25	73	32	7	35	6	11	10
.6	35	107	52	11	46	10	19	12
.8	41	129	73	13	54	14	24	17
1.0	46	183	93	17	64	20	30	22
1.5	57	289	149	26	72	31	42	35
2.0	64	391	205	35	88	37	50	47
2.5	69	535	250	42	100	-	-	-
3.0	-	625	285	45	-	-	-	-
ξ	SG NO. 10 (x = a/2, y = b/2)				SG NO. 10A (x = a/2, y = b/2)			
	MODE NO.				MODE NO.			
	1-1	1-3	3-1	3-3	1-1	1-3	3-1	3-3
.4	95	-	116	20	41	140	23	15
.6	122	15	185	32	55	186	37	22
.8	140	17	246	42	65	261	49	28
1.0	158	22	320	52	75	332	62	35
1.5	188	42	491	75	95	543	99	53
2.0	225	50	650	93	114	725	130	67
2.5	252	67	800	120	122	-	-	-
3.0	-	80	950	143	-	-	-	-
ξ	SG NO. 11 (x = 3a/8, y = b/2)				SG NO. 12 (x = a/4, y = b/2)			
	MODE NO.				MODE NO.			
	1-1	1-3	3-1	3-3	1-1	1-3	3-1	3-3
.4	70	-	57	10	26	18	69	15
.6	90	-	100	12	37	22	109	22
.8	110	-	139	15	45	32	152	32
1.0	127	-	179	20	52	42	196	40
1.5	161	-	279	30	65	70	296	58
2.0	189	-	371	40	75	107	395	80
2.5	215	-	-	-	85	-	-	-
3.0	-	-	-	-	-	-	-	-
ξ	SG NO. 13 (x = a/2, y = 3b/4)				SG NO. 14 (x = a/4, y = 3b/4)			
	MODE NO.				MODE NO.			
	1-1	1-3	3-1	3-3	1-1	1-3	3-1	3-3
.4	50	41	49	15	23	20	58	15
.6	65	48	81	22	32	32	100	24
.8	80	62	109	32	39	42	132	34
1.0	90	69	148	42	45	53	175	42
1.5	115	115	216	62	56	88	273	62
2.0	130	181	288	85	65	119	378	85
2.5	143	-	-	-	74	156	466	105
3.0	-	-	-	-	-	180	545	117

CHAPTER IV

COMPARISON OF CALCULATED AND EXPERIMENTAL RESULTS

The data generated in the previously described test program were compared with the analytical results to yield empirical equations for calculating dynamic stresses under harmonic loading.

Panel Damping

The panel damping is probably the most difficult of all the parameters involved in the stress calculation for which to select a value. Standard methods of damping factor selection involve experience, use of previous test data, personnel preference, etc., and result in an analytical value based on engineering judgment. As a means of eliminating possible variations in stress due to estimation of the panel damping, a study of measured panel damping was conducted. Damping factors were determined from the measured data by the half-power method[23] and found to contain a significant amount of scatter.

Assuming that the damping is typical of structural damping, the equivalent viscous damping coefficient is inversly proportional to the forcing frequency,

$$C = \frac{K}{f}$$

where K is a constant of proportionality. The panel damping factor is

the ratio of actual damping to critical damping coefficients

$$\zeta = \frac{C}{C_c} = \frac{K}{C_c f} = \frac{K_1}{f}$$

Hence, the damping factor is also inversely proportional to the input frequency. The measured damping factors were plotted versus frequency on log-log scales, as shown in Figure 17. A mean value curve was fitted through the data points, as shown by the solid line. The equation of the mean value line is

$$\zeta = \frac{12.58}{f^{1.13}}$$

and, considering the scatter in the data, agrees very closely with the assumed form. Although the above relation is based on a limited amount of test data it represents a very convenient method of determining panel damping, especially when calculating natural frequencies and dynamic stresses on a computer, since the frequencies must first be calculated to establish the damping. A review of the literature for similar results produced a report by Jacobs and Lagerquist(24) which contains an identical plot of panel damping versus frequency. For comparison, the mean value curve from Reference (24) is plotted on Figure 17 and shows reasonable agreement.

Comparison of Dynamic Stresses

As noted on the spectrum plots and the data of Tables 3 and 4, most of the strain gages measured lower stresses in the fundamental than in the higher modes, contrary to the analytical results. At first it was thought that the mass and stiffness added to the panel

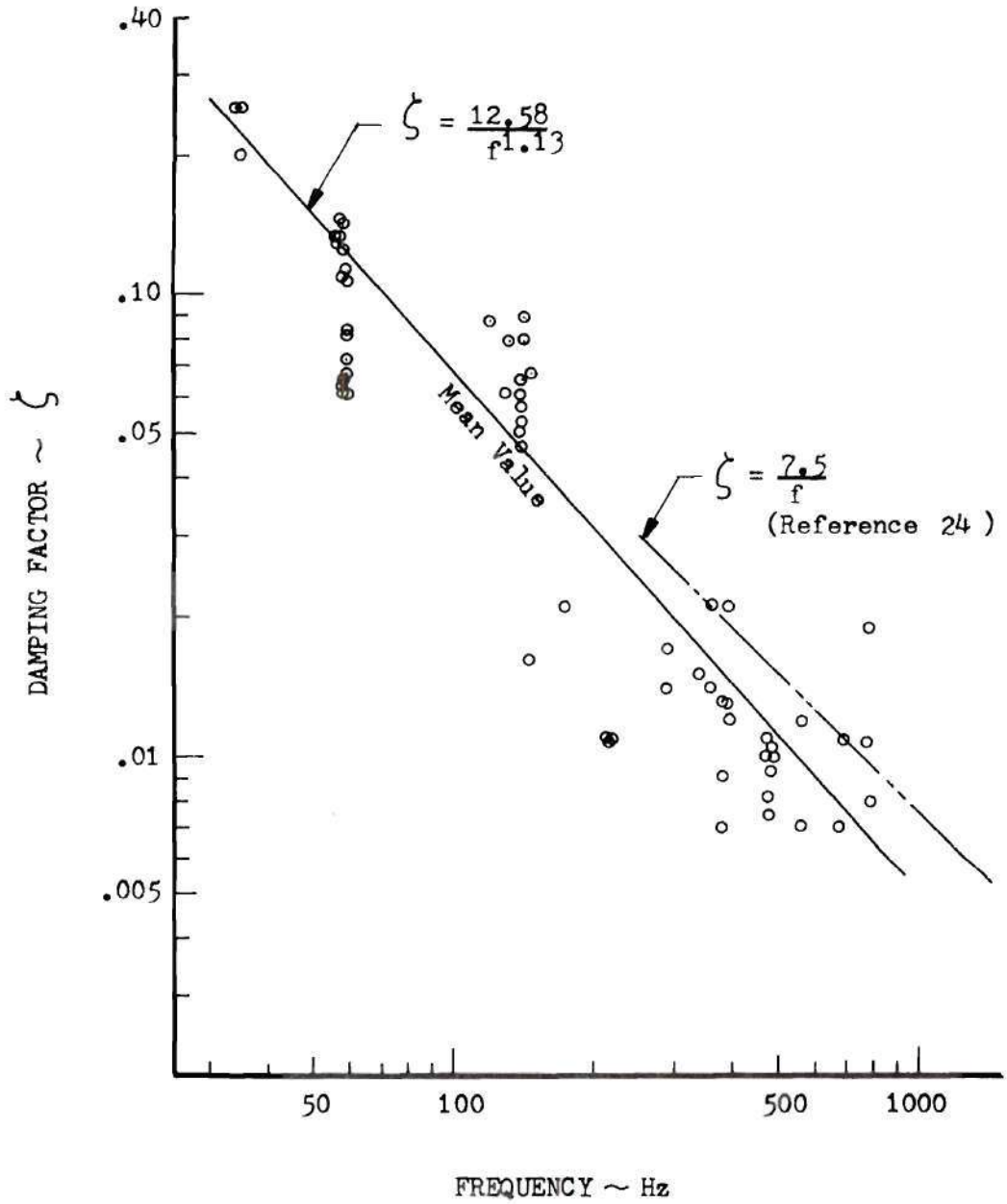

Figure 17. Panel Damping Vs. Frequency

by the strain gage installation would cause more reduction in the fundamental stress. To verify this, all but three of the strain gages were removed from the panel and the surface cleaned. The panel was subjected to the same loading conditions as in the test program and resulted in nearly identical spectrum plots. Since the strain gage installation had very little effect on measured stresses, it was concluded that the differences were due to a combination of a shift in the maximum stress location with each mode, the effect of in-plane forces introduced by the frames and the low sensitivity of the feedback loop in the shaker input which caused slow response at higher frequencies. The measured stress levels at resonance for the first four symmetric modes were plotted versus input acceleration level for each of the strain gages. The calculated results were also plotted on these curves. Through an iteration process of modifing the dynamic stress calculations and comparing them with the test results, empirical values for application to the stresses were determined. The iteration process involved trying combinations of panel parameters and mode numbers to establish a common denominator for all locations to match measured data with the calculated results. Since no combination of the above was satisfactory, the final values were established by averaging the stresses over all locations and modes.

The final empirical stress relations for the simply supported and clamped panels are given by the following modifications of the relations derived in Chapter II.

Simply Supported Panel

Equations (29) and (30) are modified to give the empirical results

$$\sigma_{X\text{-}X_{mn}} = \frac{1.68\,E\,h\,\ddot{\xi}}{a^2(1-\nu^2)\zeta\omega_{mn}^2}\left(\frac{n}{m}\right)\left[\left(\frac{a}{b}\right)^2+\nu\left(\frac{m}{n}\right)^2\right]\,SIN\,\frac{m\pi x}{a}\,SIN\,\frac{n\pi y}{b}\,e^{i(\omega T-\pi/2)}$$

$$\sigma_{Y\text{-}Y_{mn}} = \frac{1.68\,E\,h\,\ddot{\xi}}{a^2(1-\nu^2)\zeta\omega_{mn}^2}\left(\frac{n}{m}\right)\left[\left(\frac{m}{n}\right)^2+\nu\left(\frac{a}{b}\right)^2\right]\,SIN\,\frac{m\pi x}{a}\,SIN\,\frac{n\pi y}{b}\,e^{i(\omega T-\pi/2)}$$

The off-resonance stresses given by equation (28) are similarily modified by multiplying the equations by the value of 0.42.

Clamped Panel

The stresses for the clamped panel are given by equation (45) and equation (46) is modified to give

$$\{M_{X\text{-}X}\} = \frac{.30\,E\,h}{(1-\nu^2)}\left\{\beta_m^2\,U_m\,\psi_n + \nu\,\gamma_n^2\,\phi_m\,V_n\right\}$$

$$\{M_{Y\text{-}Y}\} = \frac{.30\,E\,h}{(1-\nu^2)}\left\{\gamma_n^2\,\phi_m\,V_n + \nu\,\beta_m^2\,U_m\,\psi_n\right\}$$

CONCLUSIONS AND RECOMMENDATIONS

The empirical stress functions derived in this study will be useful in predicting bounds for actual stresses and natural frequencies. This information, coupled with an applicable cumulative damage theory, will yield expected fatigue life due to multi-modal panel response.

The calculated and measured natural frequencies show reasonable agreement for all modes but the first for both the simply supported and clamped panels. The large difference in the fundamental mode is attributed in a lowering of the measured natural frequency caused by in-plane forces induced by the panel frame.

The experimental stress data shows order of magnitude agreement with the analytical results. Several of the measured stresses in the higher modes were larger than the stresses in the fundamental mode due to effects of the boundary conditions. The final empirical stress functions provide upper and lower limits for predicting stresses in actual airvehicle structural panels.

It is recommended that further research be conducted to:

(1) Expand the analytical and experimental effort to include antisymmetric loading.

(2) Analyze the stress response under random mechanical and/or acoustic loading.

(3) Evaluate the effect on fatigue life of multi-modal panel response.

(4) Investigate the preliminary panel damping versus frequency relationship established from the test data to further define the parameters which affect the damping.

APPENDIX I

PARAMETER STUDY

The effect of the various parameters on the natural frequency and maximum dynamic stress was investigated by varying each while maintaining constant values for the remaining terms. The baseline parameters chosen were those of the aluminum test specimen, as listed below:

$a = 9.0$ inches

$b = 11.0$ inches

$h = 0.032$ inches

$\nu = 0.33$

$\rho = 2.59 \times 10^{-4}$ lb.-sec.^{2}/in.^{4}

$E = 10^7$ psi

The variation of these parameters show general trends and amplitudes obtained for typical values used in the aircraft industry.

Panel Damping

The panel damping factor was varied from the mean value obtained from

$$\zeta = \frac{12.58}{f^{1.13}}$$

by increments of $\pm$ 10% ζ_{mean}.

Figure 18 depicts the effect of the damping factor on the natural frequency. Typical measured damping factors are smaller than 0.10, therefore the difference between the damped and undamped natural frequency is less than 0.25%. The damping may therefore be neglected when determining the natural frequency.

Figure 19 and 20 show the range of maximum dynamic stresses obtained by a ± 50% variation of damping factor for the simply supported and clamped panels, respectively. Both curves show a gradual decrease in stress with increasing damping factor as is expected, since the stresses are inversly proportional to the damping factor.

Panel Thickness

As shown in Figures 21 and 22, the natural frequencies very linearly with panel thickness. The maximum dynamic stresses shown in Figures 23 and 24 generally increase with increase in panel thickness while holding the input constant.

Panel Surface Dimensions

The ratio of the sides a/b was varied from 0.33 to 3 to show the effect of a/b on the natural frequency. Figures 25 thru 28 show the effect of this variation for the simply supported panel, while Figures 29 thru 32 show the same variation for the clamped panel. These curves show that, as the ratio a/b increases while b is held constant, the natural frequency approaches a limiting value. Hence, for large aspect ratio panels, the natural frequency is essentially independent of the length of the short side.

Figures 33 and 35 show the effect on the maximum stress by varying the length of the panel in the x-direction while holding b constant at the test panel dimension. As noted in the curves, this variation causes the dynamic stress to increase or decrease, according to the direction and mode of vibration. The most pronounced variation is obtained in the fundamental mode.

Figure 34 and 36 show the effect on the maximum stress obtained by varying the length in the y-direction while holding the dimension a constant at the test panel value. Again the fundamental mode stress experiences the most variation.

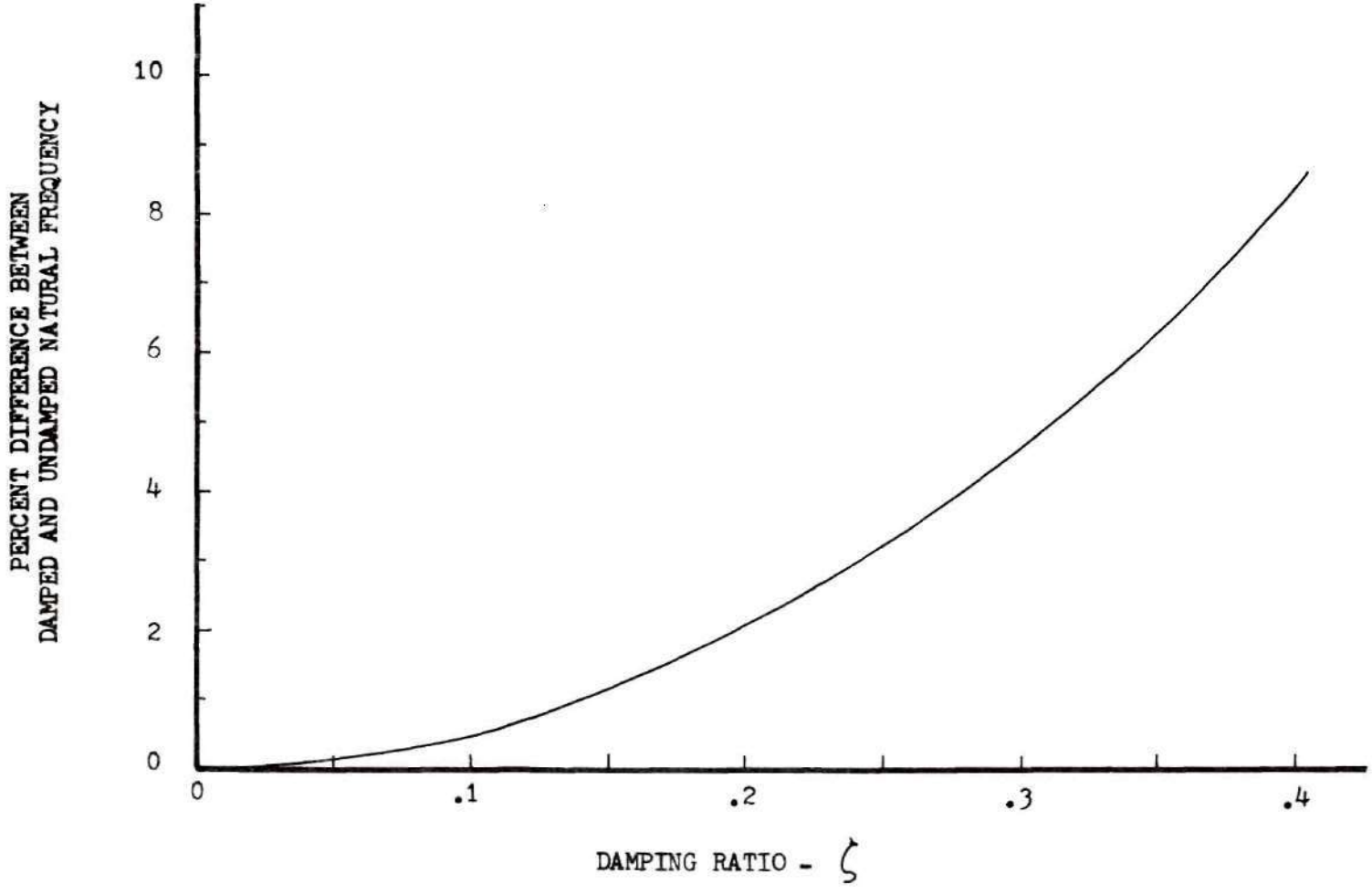

Figure 18. Effect of Damping Factor on Damped Natural Frequency

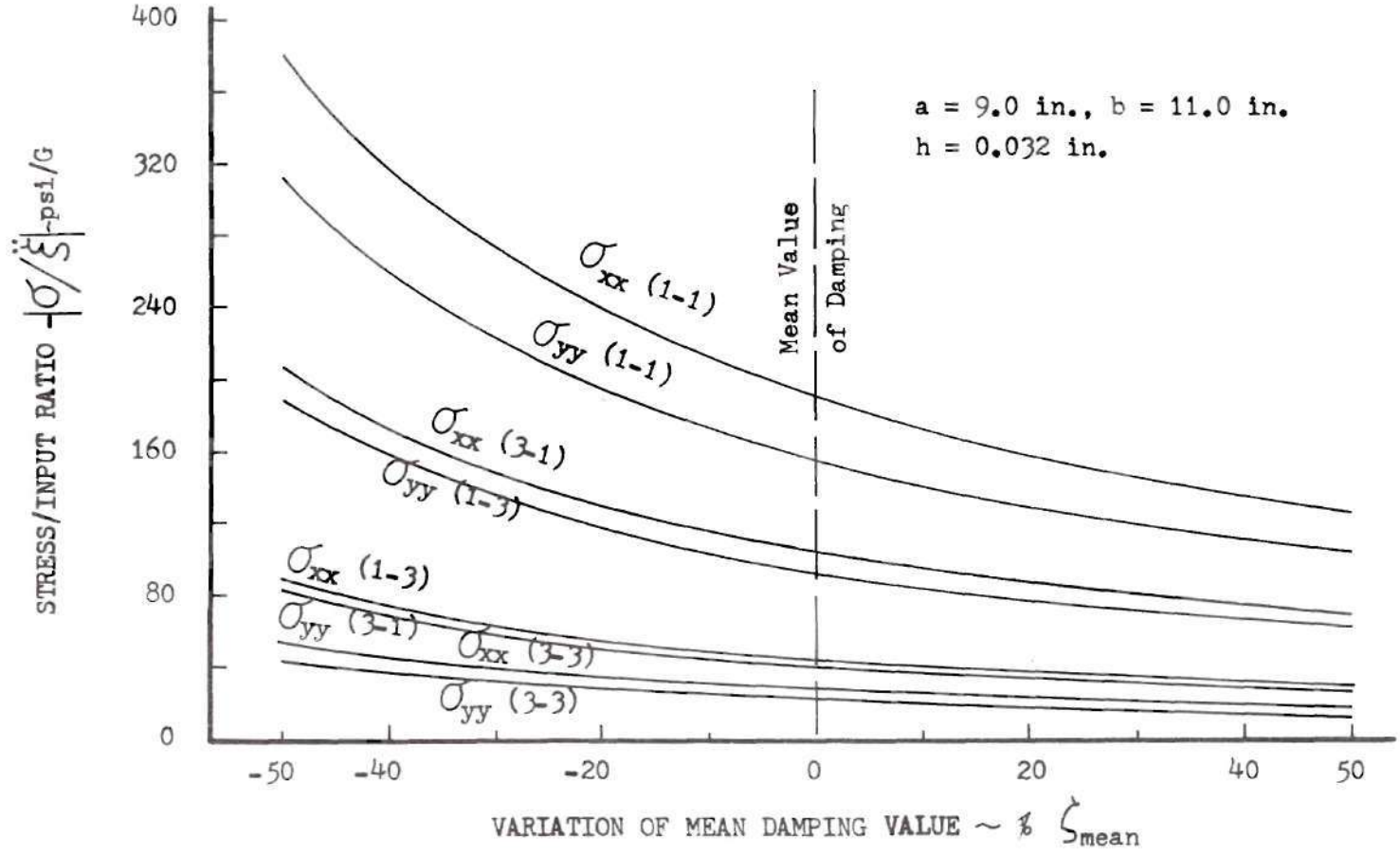

Figure 19. Effect of Damping Factor on Maximum Stress, Simply Supported Panel

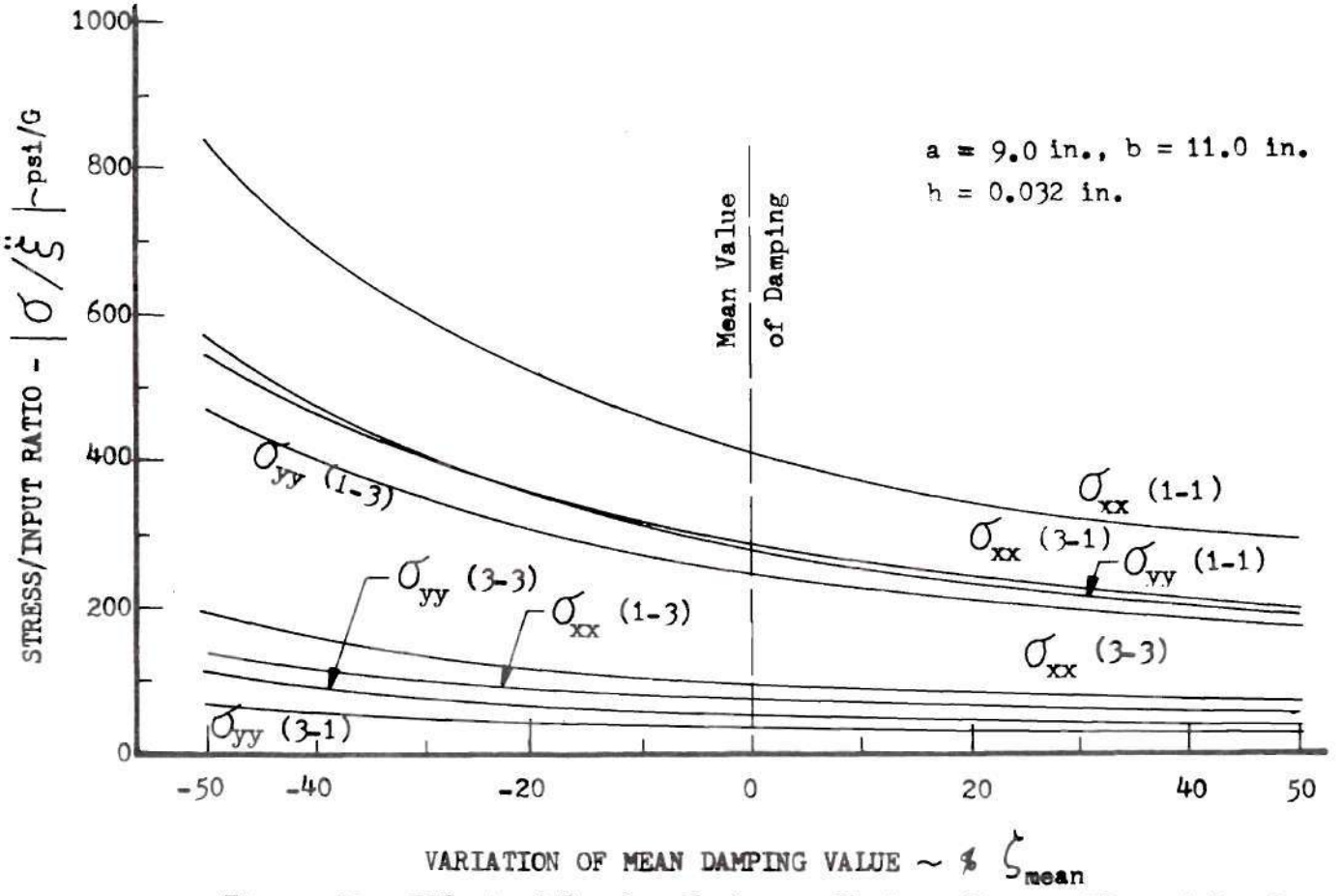

Figure 20. Effect of Damping Factor on Maximum Stress, Clamped Panel

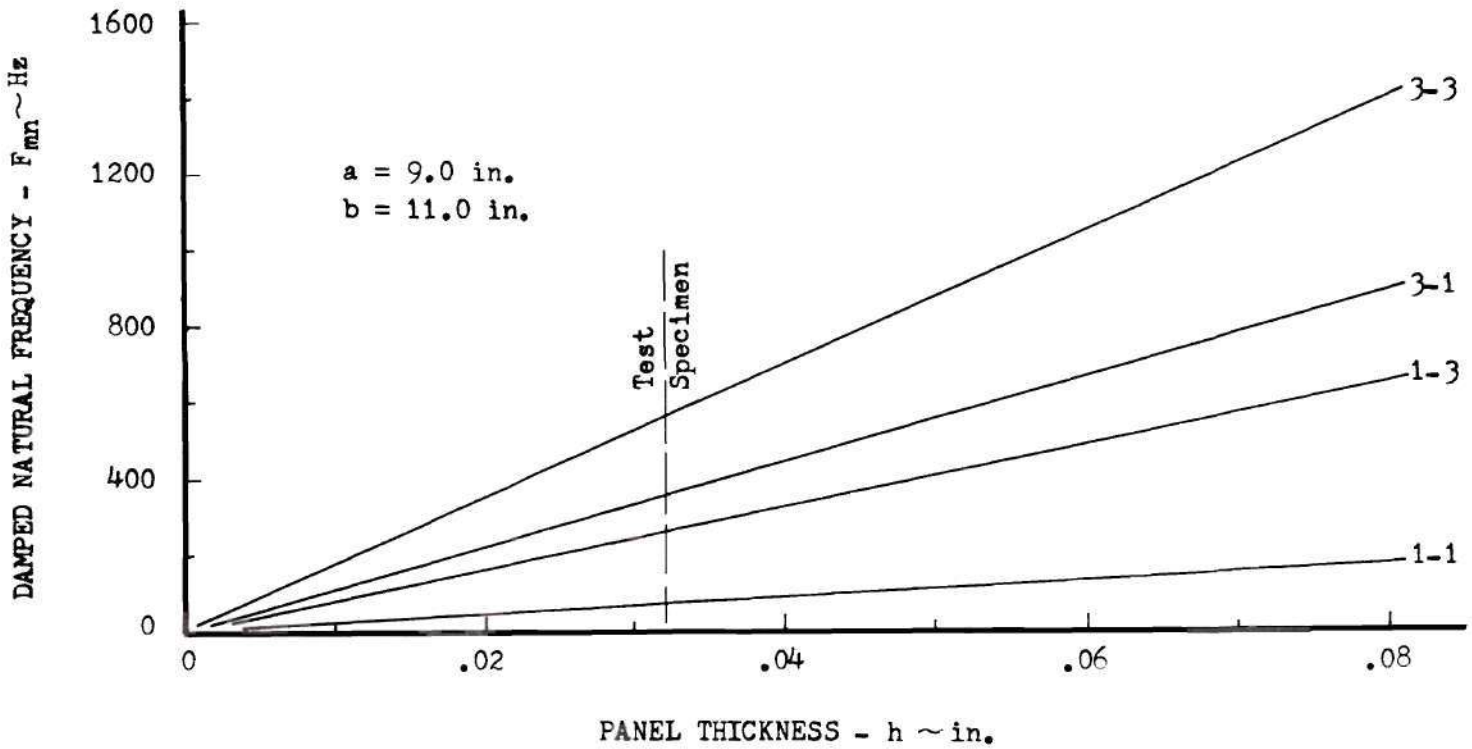

Figure 21. Effect of Panel Thickness on Natural Frequency, Simply Supported Panel

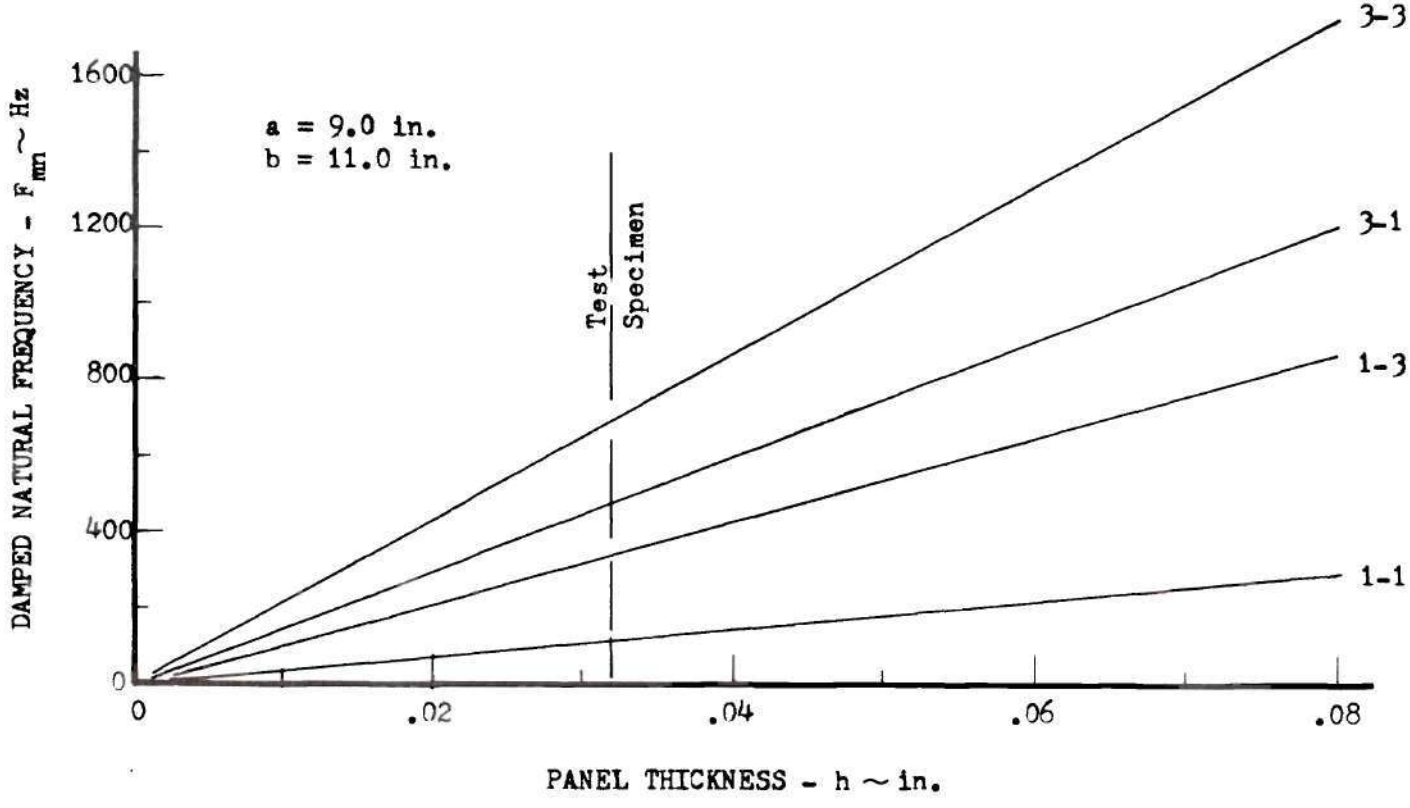

Figure 22. Effect of Panel Thickness on Natural Frequency, Clamped Panel

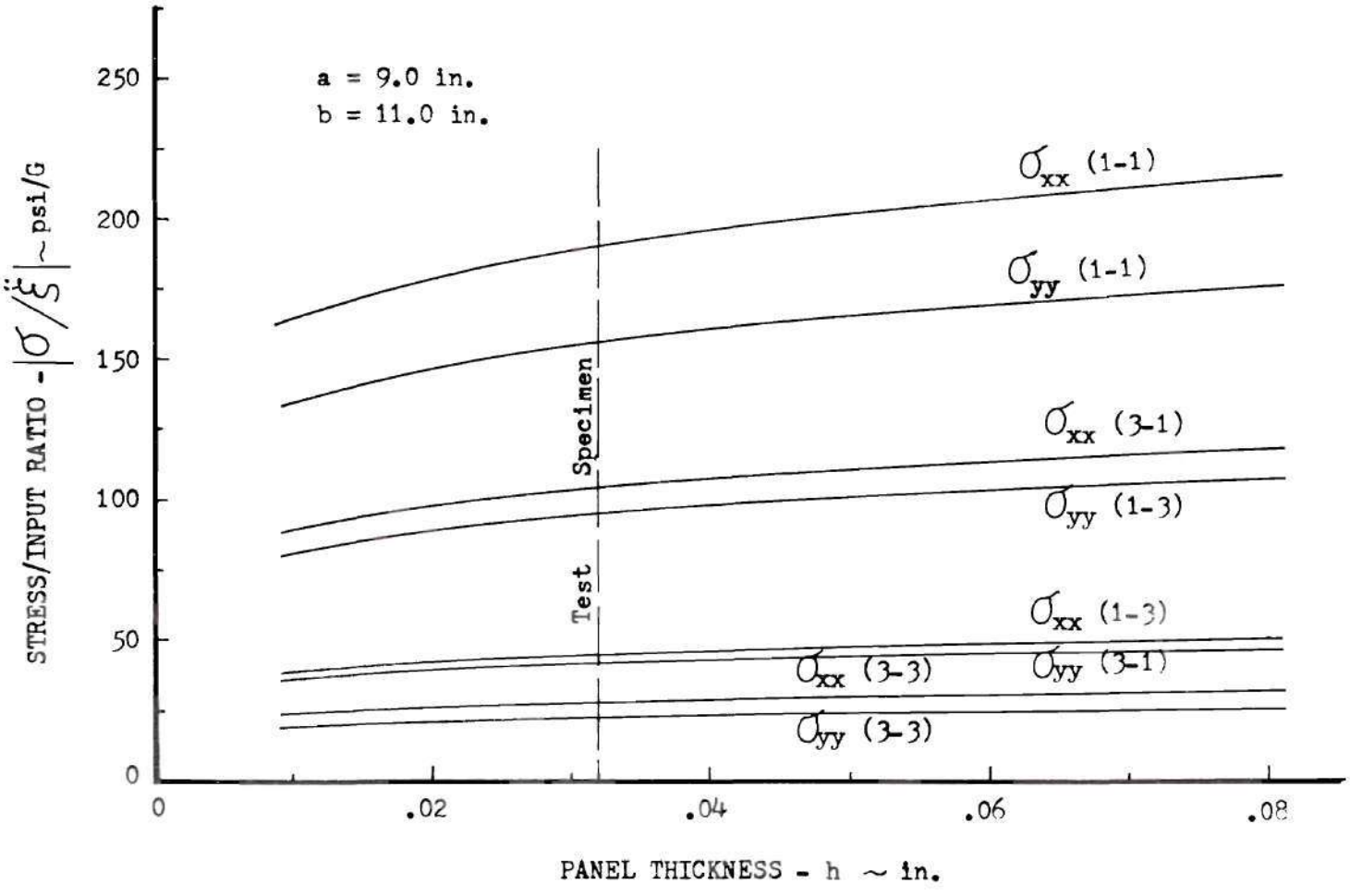

Figure 23. Effect of Panel Thickness on Maximum Stress, Simply Supported Panel

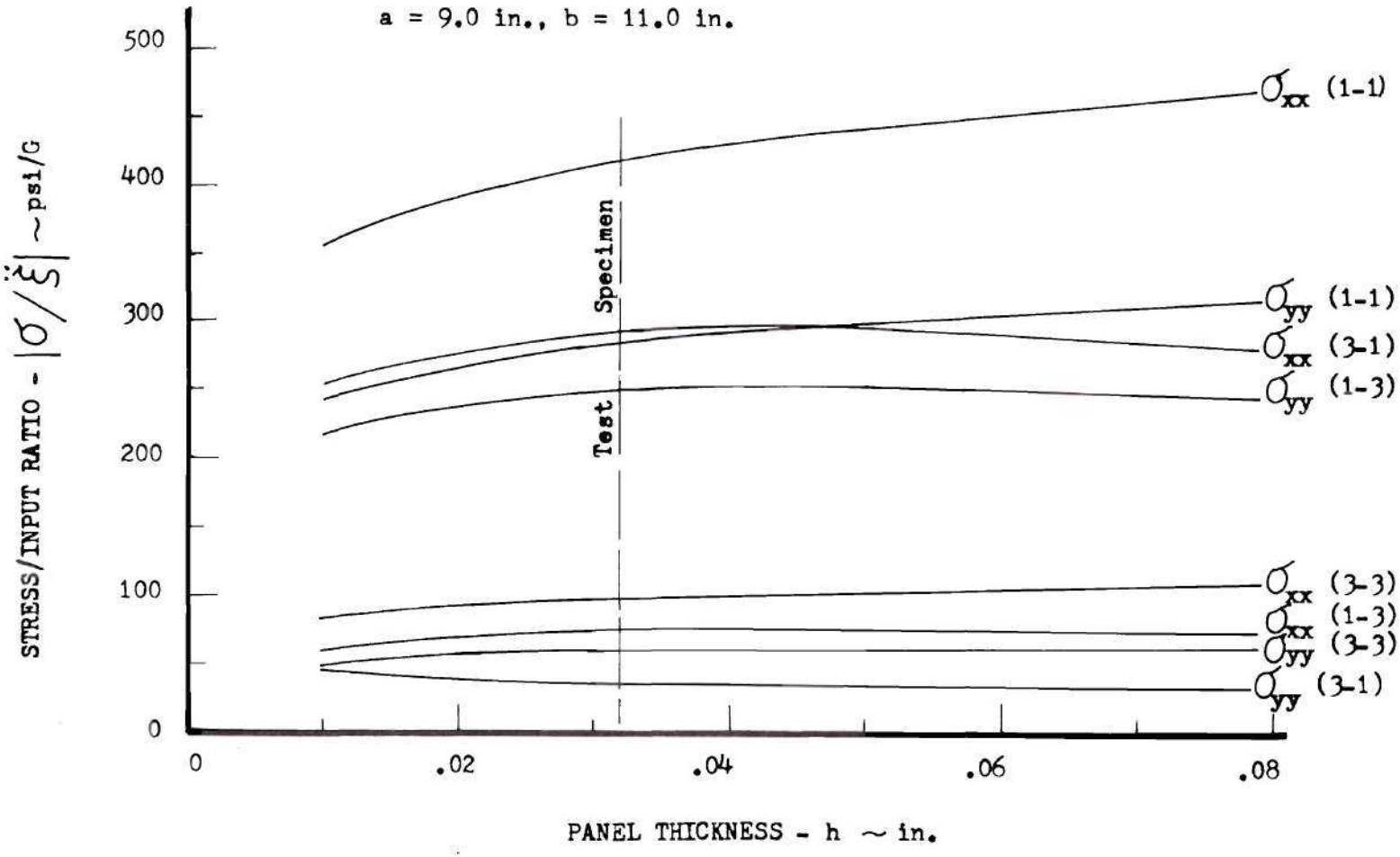

Figure 24. Effect of Panel Thickness on Maximum Stress, Clamped Panel

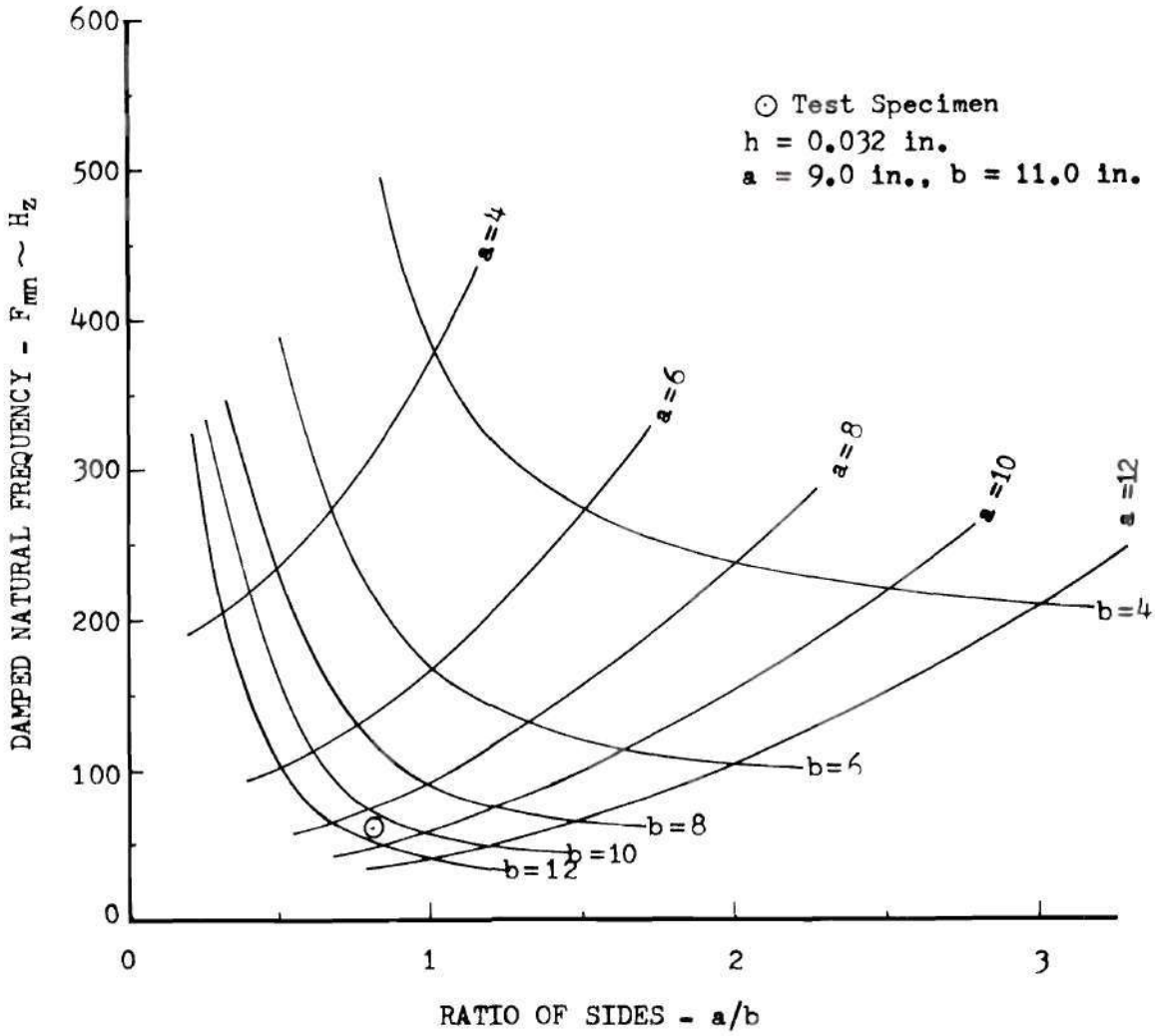

Figure 25. Effect of Ratio a/b on Natural Frequency
1-1 Mode, Simply Supported Panel

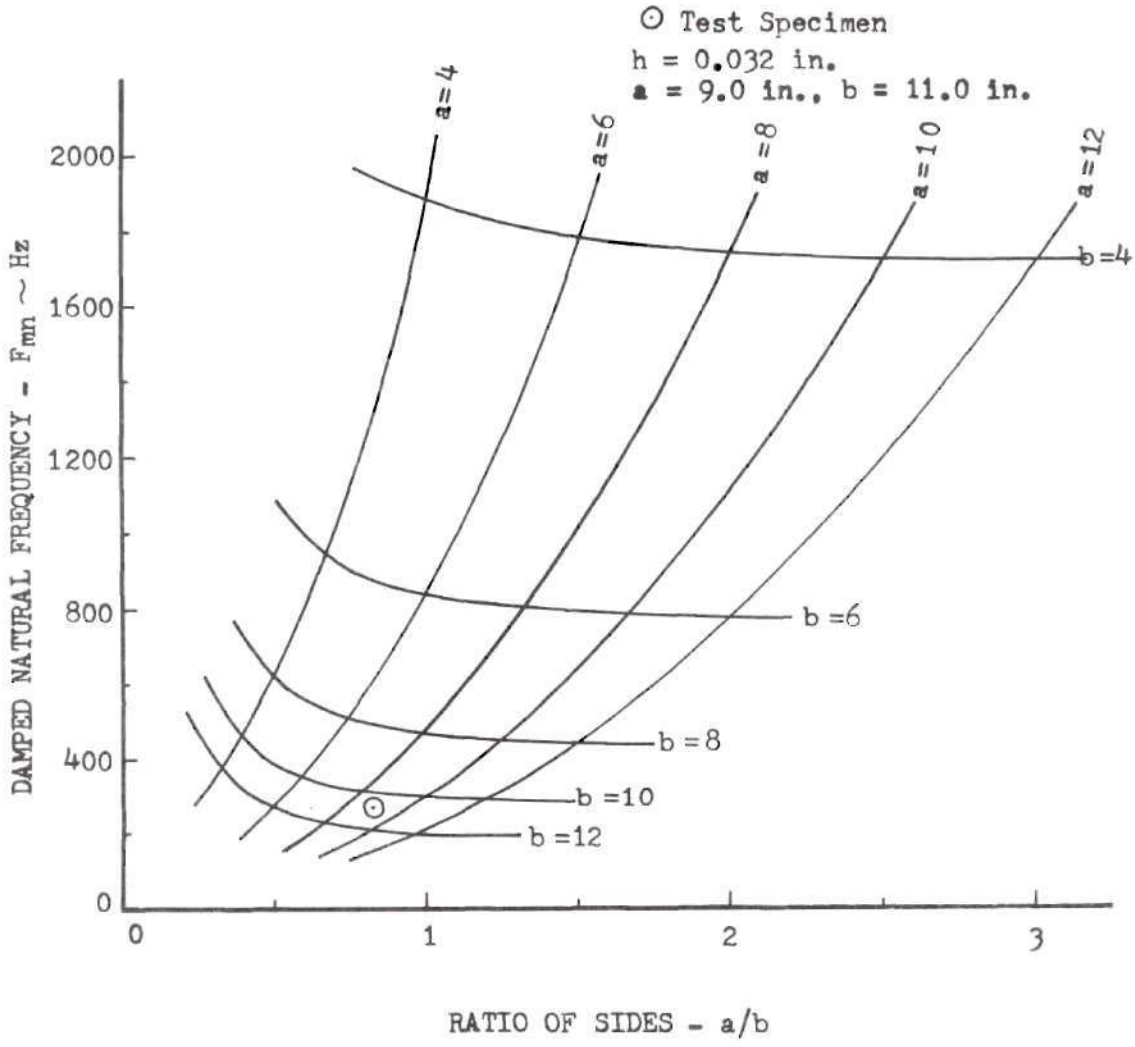

Figure 26. Effect of Ratio a/b on Natural Frequency 1-3 Mode, Simply Supported Panel

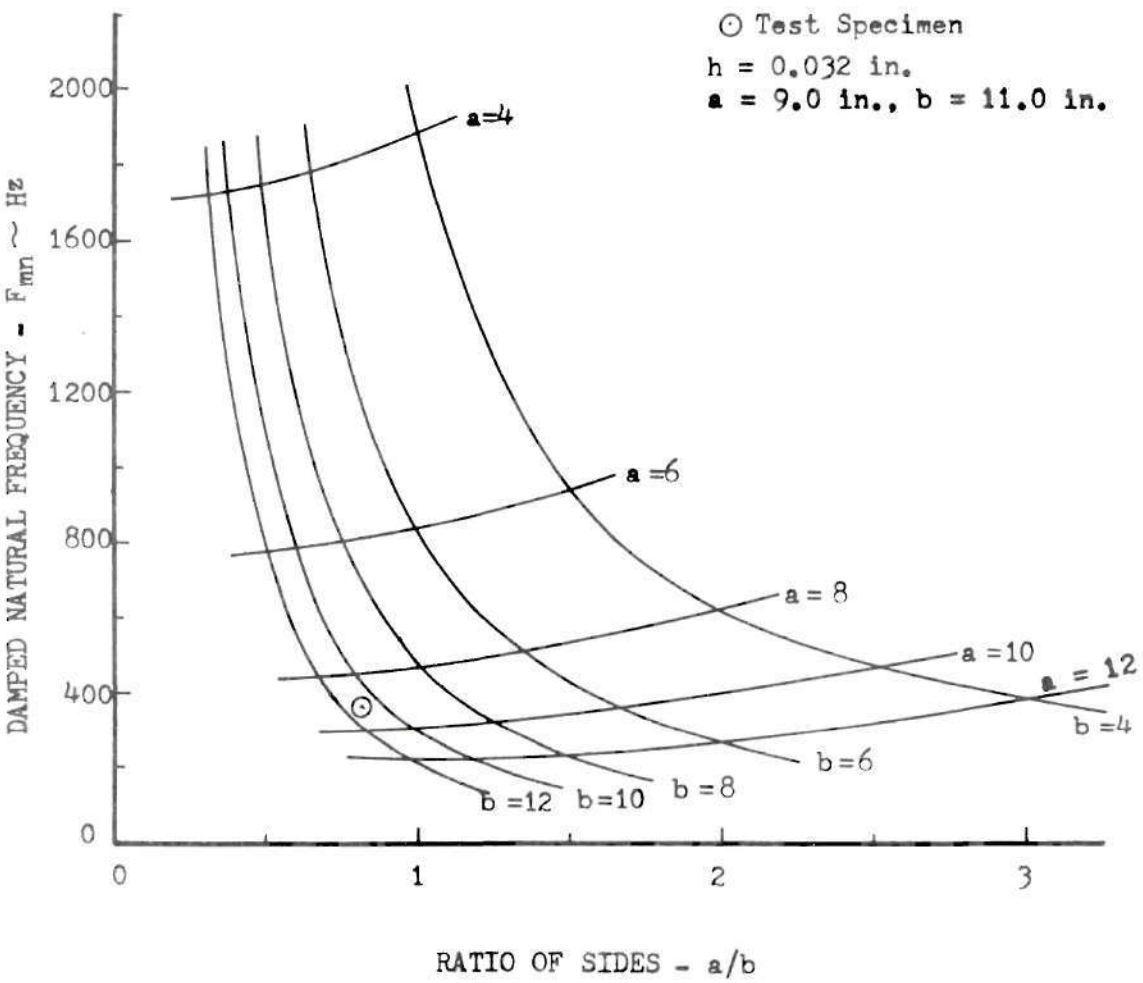

Figure 27. Effect of Ratio a/b on Natural Frequency 3-1 Mode, Simply Supported Panel

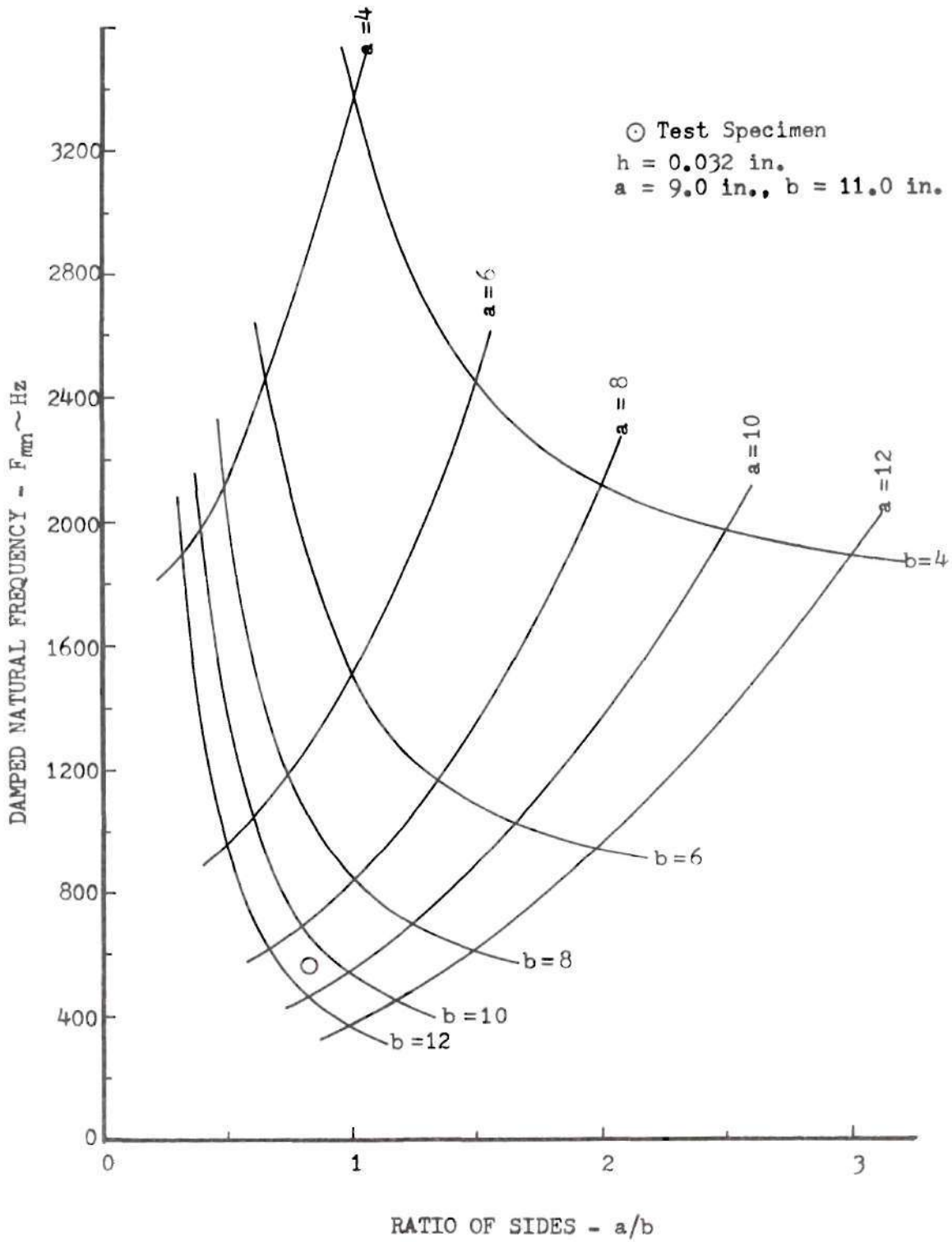

Figure 28. Effect of Ratio a/b on Natural Frequency 3-3 Mode, Simply Supported Panel

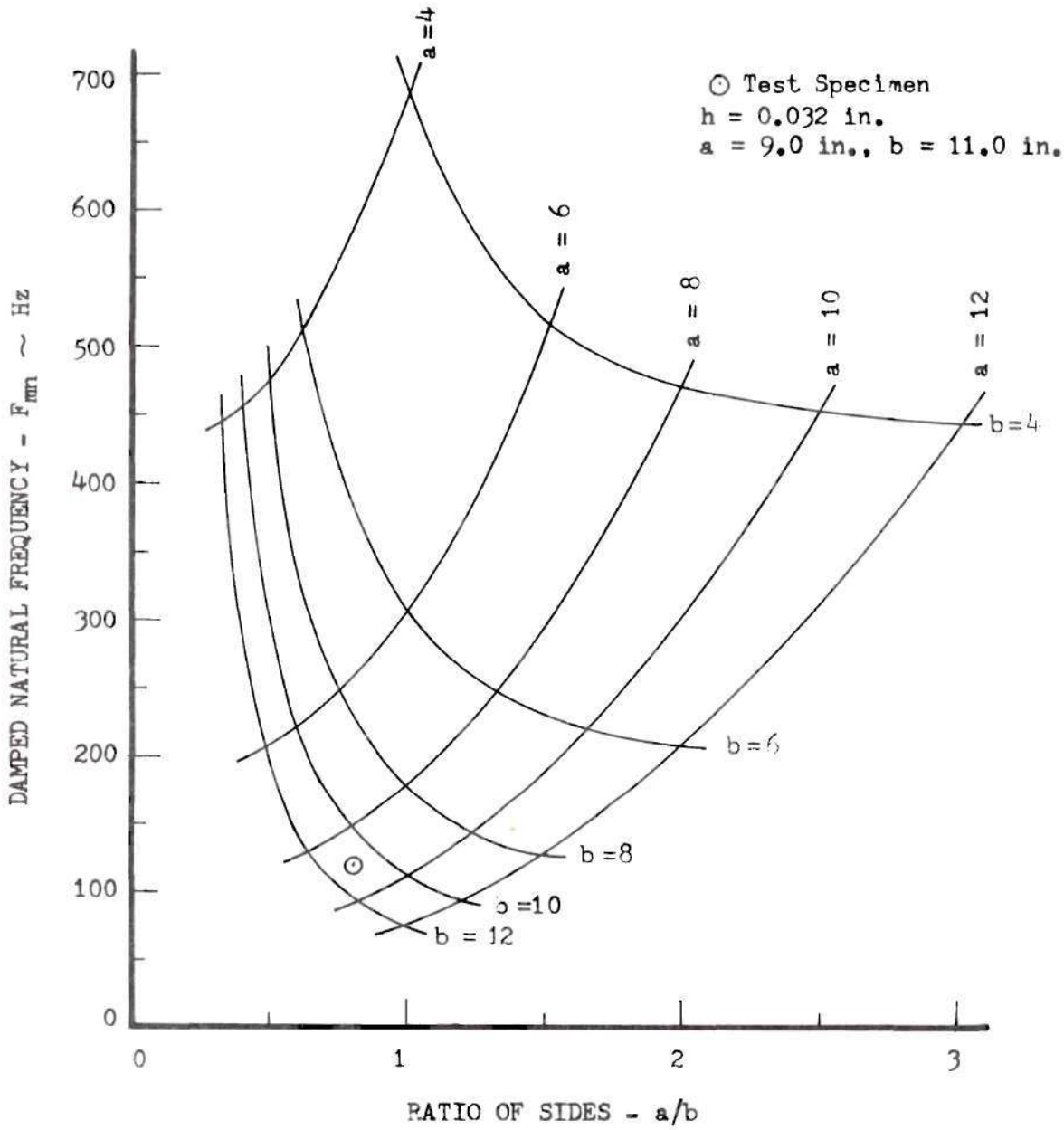

Figure 29. Effect of Ratio a/b on Natural Frequency 1-1 Mode, Clamped Panel

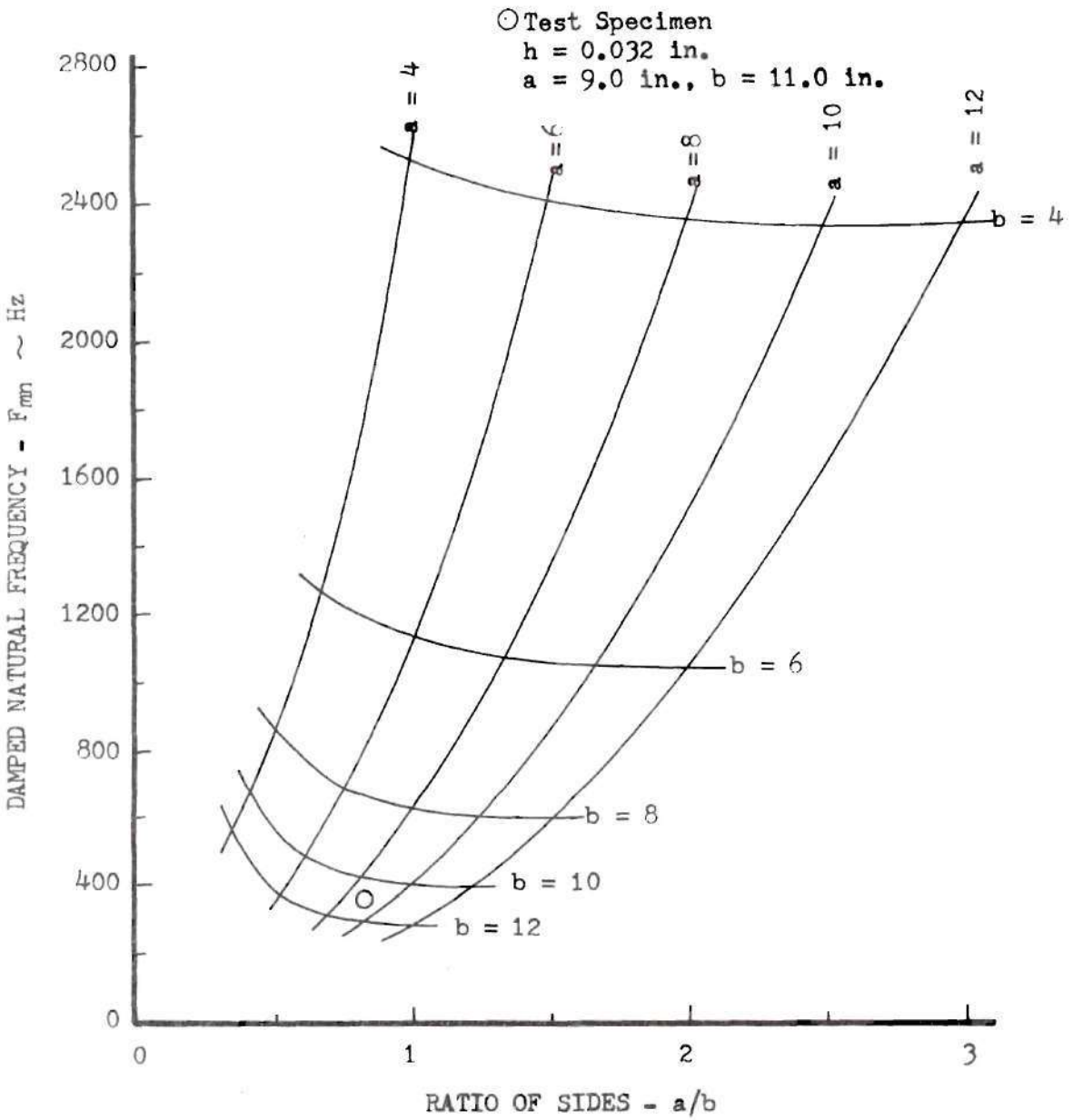

Figure 30. Effect of Ratio a/b on Natural Frequency 1-3 Mode, Clamped Panel

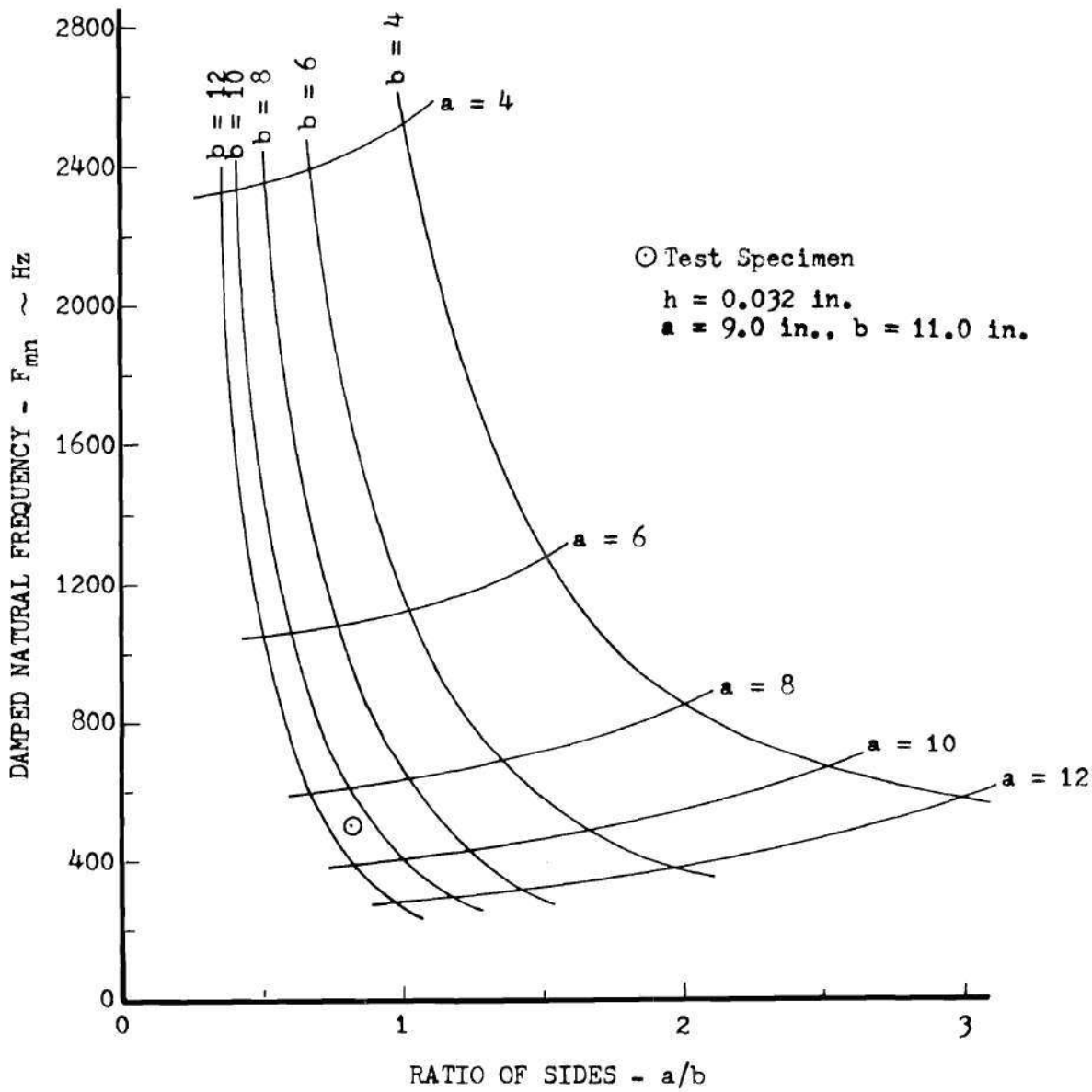

Figure 31. Effect of Ratio a/b on Natural Frequency 3-1 Mode, Clamped Panel

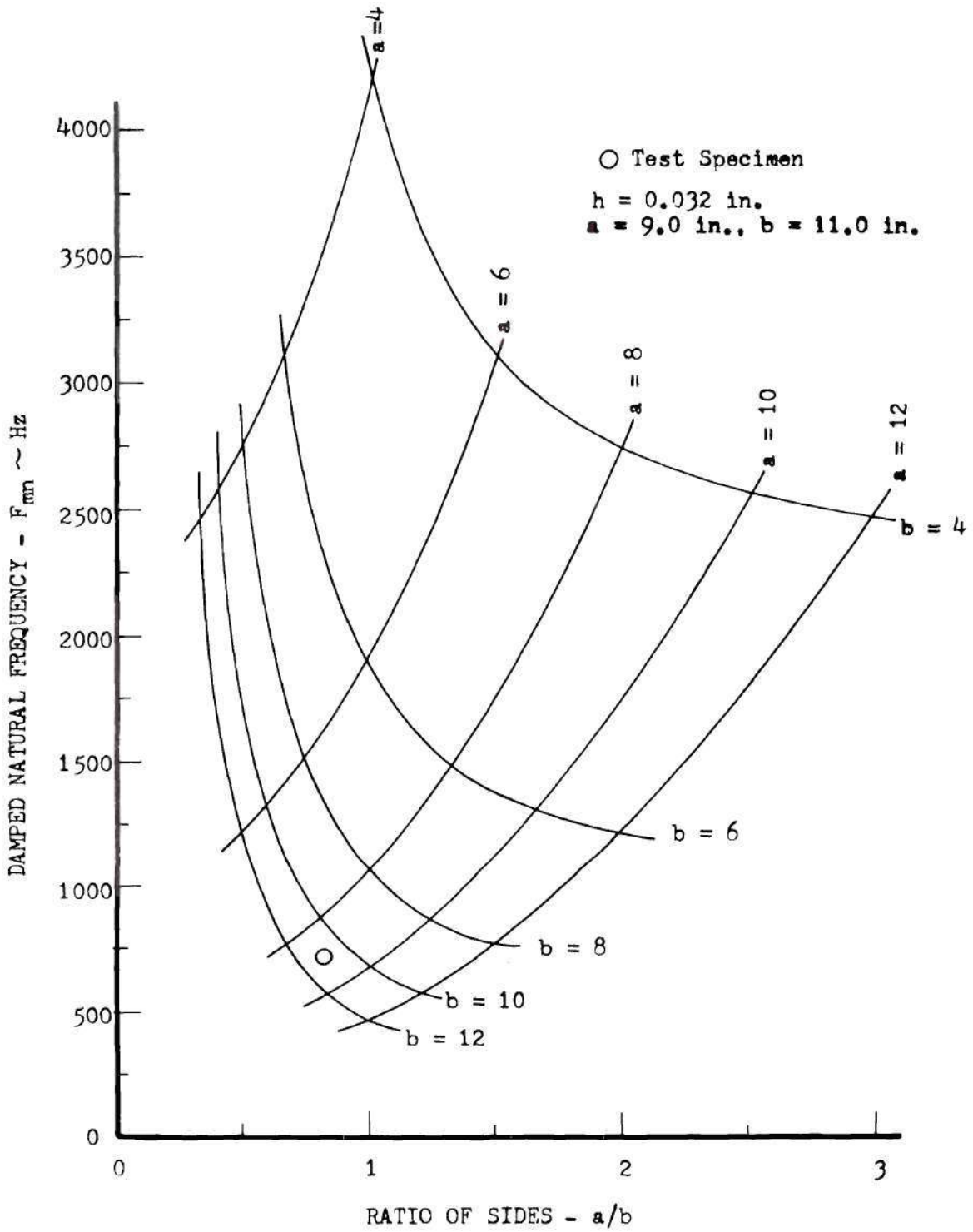

Figure 32. Effect of Ratio a/b on Natural Frequency 3-3 Mode, Clamped Panel

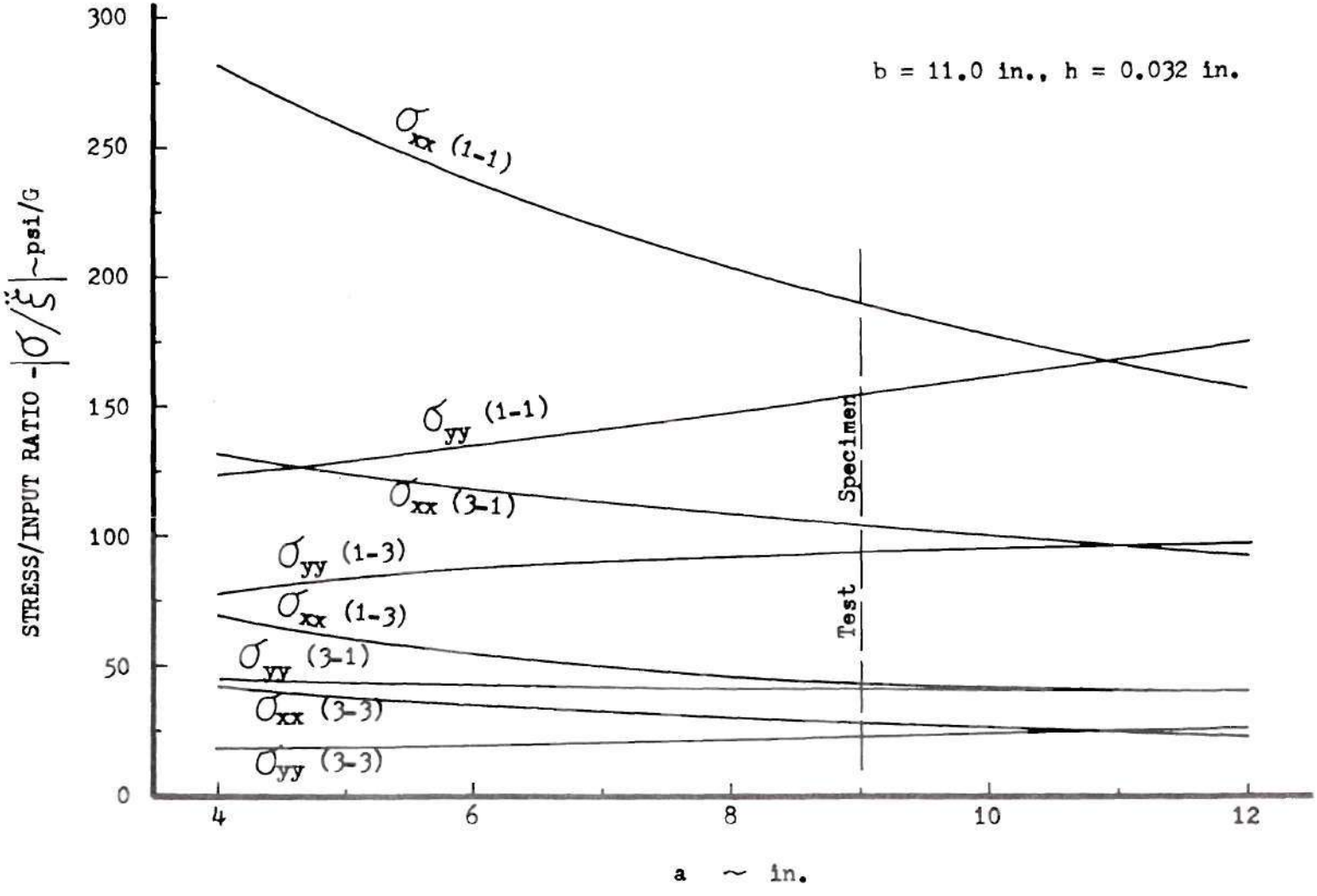

Figure 33. Effect of Panel Side "a" on Maximum Stress, Simply Supported Panel

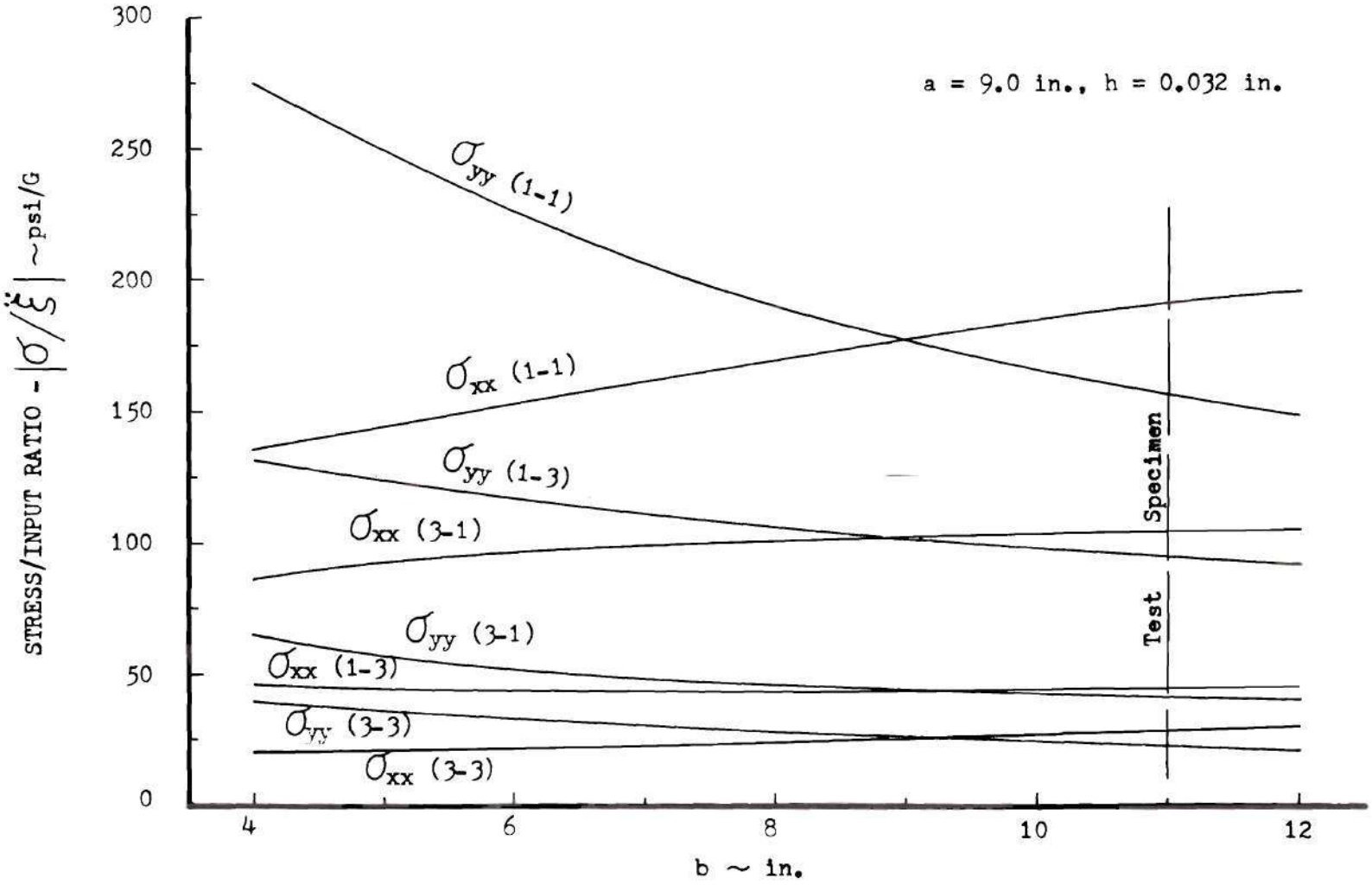

Figure 34. Effect of Panel Side "b" on Maximum Stress, Simply Supported Panel

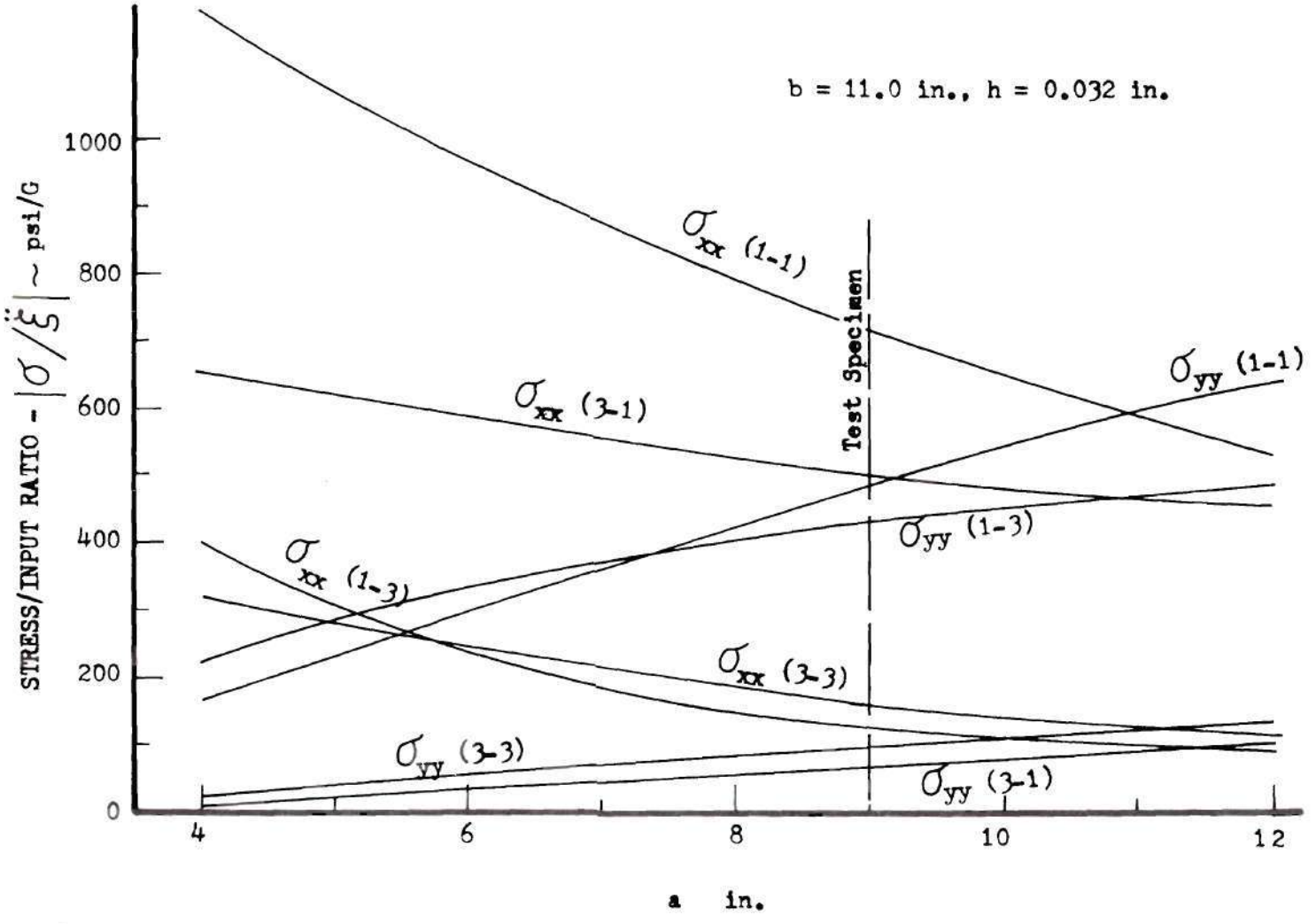

Figure 35. Effect of Panel Side "a" on Maximum Stress, Clamped Panel

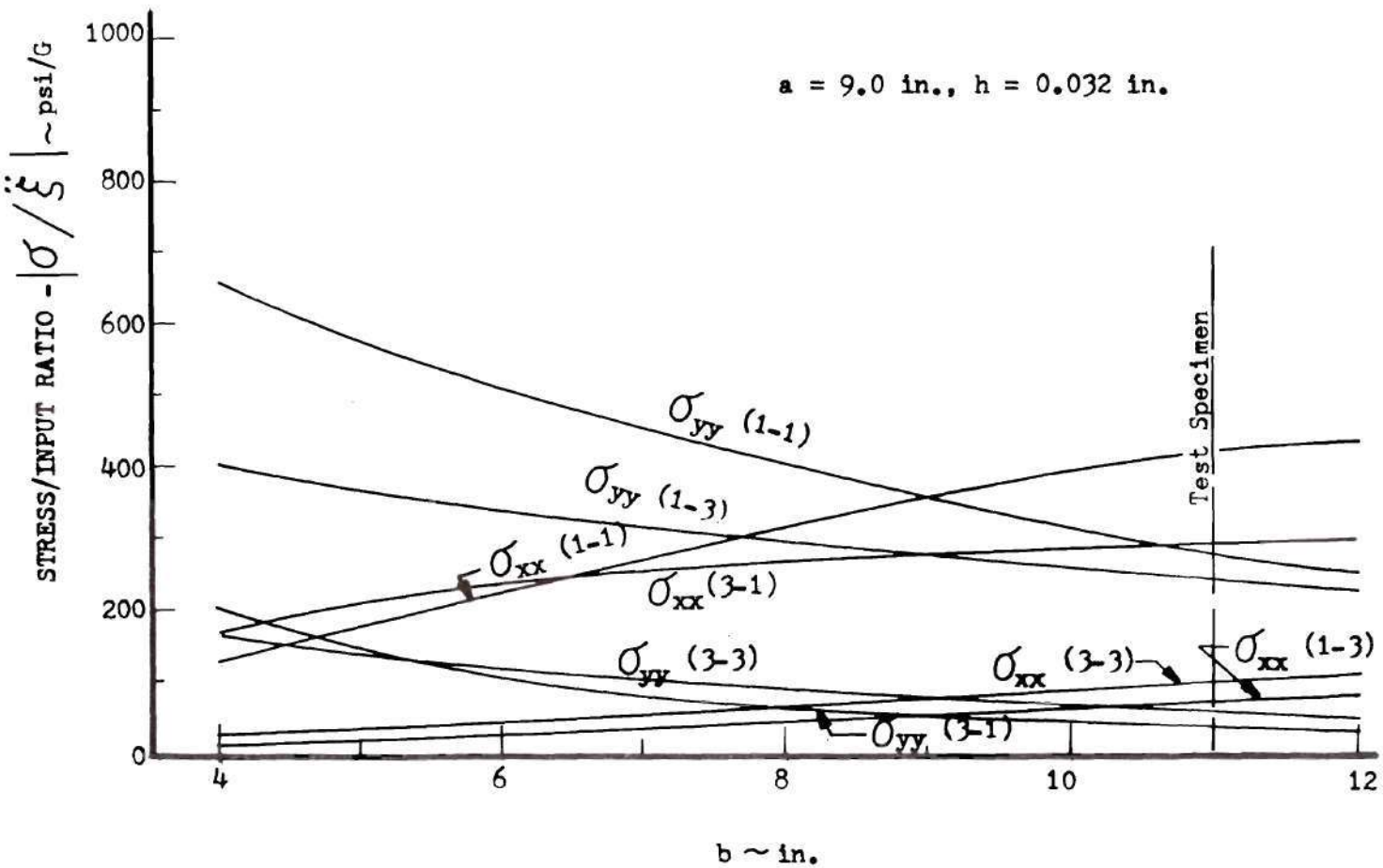

Figure 36. Effect of Panel Side "b" on Maximum Stress, Clamped Panel

APPENDIX II

COMPUTER OUTPUT

The output of the computer programs discussed in Chapter II are included in this appendix. Table 5 contains the output of the computation for the strain gage coordinates on the simply supported panel, using a one G_{rms} input acceleration. The stresses shown are in psi_{rms}. Table 6 shows the output for the clamped panel, using the same input.

Table 5. Computer Output, Simply Supported Panel

FREQUENCY-STRESS CALCULATION

9.00 IN. X 11.00 IN. X 0.0320 IN. PANEL
DENSITY= 0.100 LBS./CU.IN. POISSONS RATIO= 0.330
MODULUS OF ELASTICITY = 0.100E 08

1,1 MODE

DAMPED NATURAL FREQUENCY = 61.8 HZ. DAMPING RATIO = 0.1191

X (IN.)	Y (IN.)	ACCEL (G)	FREQ (HZ)	DELTA	SIGMA X (PSI)	SIGMA Y (PSI)	TAU (DEG)
1.50	1.83	1.000	62.2	0.1181	-0.476E 02	-0.389E 02	90.0
4.50	2.75	1.000	62.2	0.1181	-0.135E 03	-0.110E 03	90.0
2.25	2.75	1.000	62.2	0.1181	-0.953E 02	-0.780E 02	90.0
2.25	4.12	1.000	62.2	0.1181	-0.124E 03	-0.102E 03	90.0
4.50	5.50	1.000	62.2	0.1181	-0.191E 03	-0.156E 03	90.0
3.37	5.50	1.000	62.2	0.1181	-0.176E 03	-0.144E 03	90.0
2.25	5.50	1.000	62.2	0.1181	-0.135E 03	-0.110E 03	90.0
4.50	3.25	1.000	62.2	0.1181	-0.153E 03	-0.125E 03	90.0
2.25	3.25	1.000	62.2	0.1181	-0.108E 03	-0.883E 02	90.0

Table 5. (Con't)

1,3 MODE

DAMPED NATURAL FREQUENCY = 261.8 HZ. DAMPING RATIO = 0.0233

X (IN.)	Y (IN.)	ACCEL (G)	FREQ (HZ)	DELTA	SIGMA X (PSI)	SIGMA Y (PSI)	TAU (DEG)
1.50	1.83	1.000	261.9	0.0233	-0.223E 02	-0.474E 02	90.0
4.50	2.75	1.000	261.9	0.0233	-0.315E 02	-0.670E 02	90.0
2.25	2.75	1.000	261.9	0.0233	-0.223E 02	-0.474E 02	90.0
2.25	4.12	1.000	261.9	0.0233	0.119E 02	0.254E 02	90.0
4.50	5.50	1.000	261.9	0.0233	0.445E 02	0.947E 02	90.0
3.37	5.50	1.000	261.9	0.0233	0.411E 02	0.874E 02	90.0
2.25	5.50	1.000	261.9	0.0233	0.315E 02	0.670E 02	90.0
4.50	3.25	1.000	261.9	0.0233	-0.156E 02	-0.331E 02	90.0
2.25	3.25	1.000	261.9	0.0233	-0.110E 02	-0.234E 02	90.0

Table 5. (Con't)

3,1 MODE

DAMPED NATURAL FREQUENCY = 360.5 HZ. DAMPING RATIO = 0.0162

X (IN.)	Y (IN.)	ACCEL (G)	FREQ (HZ)	DELTA	SIGMA X (PSI)	SIGMA Y (PSI)	TAU (DEG)
1.50	1.83	1.000	360.5	0.0162	-0.520E 02	-0.205E 02	90.0
4.50	2.75	1.000	360.5	0.0162	0.736E 02	0.290E 02	90.0
2.25	2.75	1.000	360.5	0.0162	-0.520E 02	-0.205E 02	90.0
2.25	4.12	1.000	360.5	0.0162	-0.680E 02	-0.268E 02	90.0
4.50	5.50	1.000	360.5	0.0162	0.104E 03	0.411E 02	90.0
3.37	5.50	1.000	360.5	0.0162	0.393E 02	0.155E 02	90.0
2.25	5.50	1.000	360.5	0.0162	-0.736E 02	-0.290E 02	90.0
4.50	3.25	1.000	360.5	0.0162	0.833E 02	0.329E 02	90.0
2.25	3.25	1.000	360.5	0.0162	-0.589E 02	-0.233E 02	90.0

Table 5. (Con't)

3,3 MODE

DAMPED NATURAL FREQUENCY = 560.2 HZ. DAMPING RATIO = 0.0099

X (IN.)	Y (IN.)	ACCEL (G)	FREQ (HZ)	DELTA	SIGMA X (PSI)	SIGMA Y (PSI)	TAU (DEG)
1.50	1.83	1.000	560.2	0.0099	-0.282E 02	-0.231E 02	90.0
4.50	2.75	1.000	560.2	0.0099	0.199E 02	0.163E 02	90.0
2.25	2.75	1.000	560.2	0.0099	-0.141E 02	-0.115E 02	90.0
2.25	4.12	1.000	560.2	0.0099	0.755E 01	0.618E 01	90.0
4.50	5.50	1.000	560.2	0.0099	-0.282E 02	-0.231E 02	90.0
3.37	5.50	1.000	560.2	0.0099	-0.106E 02	-0.871E 01	90.0
2.25	5.50	1.000	560.2	0.0099	0.199E 02	0.163E 02	90.0
4.50	3.25	1.000	560.2	0.0099	0.985E 01	0.806E 01	90.0
2.25	3.25	1.000	560.2	0.0099	-0.696E 01	-0.570E 01	90.0

Table 6. Computer Output, Clamped Panel

FREQUENCY-STRESS CALCULATION

9.00 IN.X 11.00 IN.X 0.0320 IN. PANEL
DENSITY= 0.100 LBS./CU.IN. POISSONS RATIO= 0.330
MODULUS OF ELASTICITY = 0.100E 08

1,1 MODE

DAMPED NATURAL FREQUENCY = 114.5 HZ. DAMPING RATIO = 0.0593

1,3 MODE

DAMPED NATURAL FREQUENCY = 350.6 HZ. DAMPING RATIO = 0.0167

3,1 MODE

DAMPED NATURAL FREQUENCY = 483.4 HZ. DAMPING RATIO = 0.0117

3,3 MODE

DAMPED NATURAL FREQUENCY = 700.9 HZ. DAMPING RATIO = 0.0077

Table 6. (Con't)

X (IN.)	Y (IN.)	ACCEL (G)	FREQ (HZ)	DELTA	SIGMA X (PSI)	TAU (DEG)	SIGMA Y (PSI)	TAU (DEG)
4.50	0.0	1.000	114.7	0.0592	0.933E 02	-88.4	0.283E 03	-88.4
			350.7	0.0167	0.830E 02	88.4	0.251E 03	88.4
			483.5	0.0117	0.129E 02	-70.7	0.392E 02	-70.7
			700.9	0.0077	0.188E 02	-87.0	0.568E 02	-87.0
2.25	0.0	1.000	114.7	0.0592	0.509E 02	-87.4	0.154E 03	-87.4
			350.7	0.0167	0.460E 02	-89.9	0.139E 03	-89.9
			483.5	0.0117	0.117E 02	81.6	0.356E 02	81.6
			700.9	0.0077	0.117E 02	85.5	0.355E 02	85.5
0.0	2.75	1.000	114.7	0.0592	0.229E 03	-88.1	0.755E 02	-88.1
			350.7	0.0167	0.595E 02	-84.1	0.196E 02	-84.1
			483.5	0.0117	0.171E 03	89.2	0.563E 02	89.2
			700.9	0.0077	0.496E 02	84.2	0.164E 02	84.2
0.0	5.50	1.000	114.7	0.0592	0.417E 03	-89.5	0.138E 03	-89.5
			350.7	0.0167	0.768E 02	84.8	0.253E 02	84.8
			483.5	0.0117	0.302E 03	89.5	0.998E 02	89.5
			700.9	0.0077	0.957E 02	-85.9	0.316E 02	-85.9
1.50	1.83	1.000	114.7	0.0592	0.347E 02	87.1	0.281E 02	85.7
			350.7	0.0167	0.370E 01	-8.7	0.371E 02	-87.6
			483.5	0.0117	0.477E 02	-88.3	0.101E 02	88.9
			700.9	0.0077	0.403E 02	88.7	0.338E 02	89.1

Table 6. (Con't)

X (IN.)	Y (IN.)	ACCEL (G)	FREQ (HZ)	DELTA	SIGMA X (PSI)	TAU (DEG)	SIGMA Y (PSI)	TAU (DEG)
4.50	2.75	1.000	114.7	0.0592	0.146E 03	89.9	0.761E 02	-86.5
			350.7	0.0167	0.866E 02	83.9	0.170E 03	88.5
			483.5	0.0117	0.125E 03	-87.4	0.456E 02	-79.5
			700.9	0.0077	0.507E 02	88.6	0.503E 02	-88.6
2.25	2.75	1.000	114.7	0.0592	0.297E 02	-80.9	0.252E 02	-78.6
			350.7	0.0167	0.363E 02	-80.9	0.904E 02	-88.5
			483.5	0.0117	0.108E 03	89.8	0.404E 02	86.4
			700.9	0.0077	0.397E 02	86.0	0.339E 02	86.7
2.25	4.12	1.000	114.7	0.0592	0.615E 02	-86.7	0.833E 02	-89.5
			350.7	0.0167	0.128E 02	56.9	0.230E 02	85.2
			483.5	0.0117	0.171E 03	89.7	0.696E 02	89.9
			700.9	0.0077	0.266E 02	-82.0	0.147E 02	-84.2
4.50	5.50	1.000	114.7	0.0592	0.302E 03	88.6	0.246E 03	88.1
			350.7	0.0167	0.101E 03	-82.3	0.198E 03	-88.1
			483.5	0.0117	0.227E 03	88.9	0.938E 02	85.3
			700.9	0.0077	0.905E 02	-86.9	0.713E 02	-87.3
3.37	5.50	1.000	114.7	0.0592	0.241E 03	89.2	0.207E 03	88.3
			350.7	0.0167	0.861E 02	-86.5	0.173E 03	-88.8
			483.5	0.0117	0.469E 02	87.4	0.209E 02	74.5
			700.9	0.0077	0.222E 02	-87.0	0.215E 02	-85.5

Table 6. (Con't)

X (IN.)	Y (IN.)	ACCEL (G)	FREQ (HZ)	DELTA	SIGMA X (PSI)	TAU (DEG)	SIGMA Y (PSI)	TAU (DEG)
2.25	5.50	1.000	114.7	0.0592	0.733E 02	-88.3	0.104E 03	88.6
			350.7	0.0167	0.452E 02	81.0	0.107E 03	89.2
			483.5	0.0117	0.195E 03	89.7	0.798E 02	-88.7
			700.9	0.0077	0.717E 02	-86.9	0.491E 02	-89.0
4.50	3.25	1.000	114.7	0.0592	0.194E 03	89.5	0.130E 03	-88.9
			350.7	0.0167	0.585E 02	79.2	0.115E 03	87.3
			483.5	0.0117	0.155E 03	-88.4	0.602E 02	-84.2
			700.9	0.0077	0.270E 02	85.7	0.310E 02	-89.2
2.25	3.25	1.000	114.7	0.0592	0.431E 02	-83.9	0.501E 02	-85.4
			350.7	0.0167	0.243E 02	-74.7	0.609E 02	-87.8
			483.5	0.0117	0.135E 03	89.8	0.531E 02	87.8
			700.9	0.0077	0.210E 02	81.1	0.207E 02	84.6

REFERENCES

(1) S. Tomotika, "The Transverse Vibration of a Square Plate Clamped at Four Edges", Philosophical Magazine, Series 7, Vol. 21, No. 142, April 1936, pp 745 - 760.

(2) D. Young, "Vibration of Rectangular Plates by the Ritz Method", Journal of Applied Mechanics, Vol. 17, 1950, pp 448 - 453.

(3) G. B. Warburton, "The Vibration of Rectangular Plates", Proceedings of the Institute of Mechanical Engineers, Vol. 168, 1954.

(4) M. Levy, "Sur 1'equilibre elastique d'une plaque rectangularie", Comptes Rendus, Vol. 129, 1899, pp 535 - 539.

(5) N. J. Huffington and W. H. Hoppmann, "On the Transverse Vibrations of Rectangular Orthotropic Plates", Journal of Applied Mechanics, Vol. 25, Trans. ASME, Vol. 80, 1958, pp 389 - 395.

(6) R.F.S. Hearmon, "The Frequency of Flexural Vibration of Rectangular Orthotropic Plates with Clamped or Supported Edges", Journal of Applied Mechanics, Trans. ASME, Vol. 26, 1959, pp 537 - 540.

(7) B. Y. Ballal, "Vibrations of Rectangular Plates", Masters Thesis, Rice University, July 1966.

(8) P. A. Laura and B. F. Saffell, "Study of Small-Amplitude Vibrations of clamped Rectangular Plates Using Polynominal Approximations", Journal of the Acoustical Society of America, Vol. 41, No. 4, 1967, pp 836 - 839.

(9) R. D. Ford, "Response of a Model Structure to Noise - Part I, Flat Panels", ASD-TRD-62-706, July 1962.

(10) C. A. Mercer and C. Seavey, "Prediction of Natural Frequencies and Normal Modes of Skin-Stringer Panel Rows", Journal of Sound and Vibration, Vol. 6, No. 1, 1967, pp 139 - 162.

(11) Y. K. Lin, "Stresses in Continuous Skin-Stiffener Panels Under Random Loading", Journal of the Aerospace Sciences, Vol. 29, 1962, pp 67 - 75.

(12) Y. K. Lin, "Free Vibration of Continuous Skin-Stringer Panels", Journal of Applied Mechanics, Vol. 27, 1960, pp 669 - 676.

(13) B. L. Clarkson, "Stresses in Skin Panels Subjected to Random Acoustic Loadings", Air Force Materials Laboratory Technical Report AFML-TR-67-199, June 1967.

(14) J. R. Ballentine, F. F. Rudder, J. T. Mathis, and H. E. Plumblee, "Refinement of Sonic Fatigue Structural Design Criteria". Air Force Flight Dynamics Laboratory Technical Report AFFDL-TR-67-156. Nov. 1967.

(15) W. Nowacki, Dynamics of Elastic Systems, John Wiley & Sons, 1963.

(16) L. Meirovitch, Analytical Methods in Vibrations, The MacMillan Co. 1967.

(17) S. Timoshenko and S. Woinowsky-Krieger, Theory of Plates and Shells, McGraw-Hill, 1959.

(18) D. Young and R. P. Felger, "Tables of Characteristic Functions Representing Normal Modes of Vibration of Beam", Engineering Research Bulletin No. 4913, Bureau of Engineering Research, University of Texas, 1949.

(19) R. Courant and D. Hilbert, Methods of Mathematical Physics, Volume 1, Interscience Publishers, Inc. 1953.

(20) R. M. Scruggs, "Transverse Vibration of a Cantilevered Circular Cylindrical Shell", Masters Thesis, Department of Engineering Mechanics, Georgia Institute of Technology, June 1964.

(21) R. P. Felgar, "Formulas for Integrals Containing Characteristic Functions of a Vibrating Beam", Circular No. 14, Bureau of Engineering Research, University of Texas, Austin, 1950.

(22) J. R. Ballentine, H. E. Plumblee, and C. W. Schneider, "Sonic Fatigue in Compined Environment", Air Force Flight Dynamics Laboratory Technical Report AFFDL-TR-66-7, May 1966.

(23) W. T. Thompson, Vibration Theory and Applications, Prentice-Hall, Inc. 1965.

(24) L. D. Jacobs and D. R. Lagerquist, "A Finite Element Analysis and Simple Panel Response to Turbulent Boundary Layers", Air Force Flight Dynamics Laboratory Technical Report AFFDL-TR-67-81, December 1967.